APPENDIX I. PHYSICAL PROPERTIES AND CORRELATION OF SEISMIC PROFILES WITH DRILLING RESULTS[1]

Lucien Montadert, Institut Français du Pétrole
and
C. Wylie Poag, U.S. Geological Survey, Woods Hole[2]

INTRODUCTION

The data and interpretations presented in this appendix are chiefly the results of shipboard investigations and should be considered preliminary. Additional analyses and subsequent interpretations can be found in Part VIII of this volume (Masson et al.; Scrutton; Sibuet et al.; and see also Maury et al.).

SITE 548

Physical Properties

For Holes 548 and 548A four physical properties were measured on undisturbed samples taken every two sections: (a) sound velocity with the Hamilton Frame (we acquired a sufficient number of velocity measurements to establish a detailed log which correlates well with downhole logs); (b) wet-bulk density with the GRAPE special 2-minute count; (c) wet-bulk-density water content (two values of wet-bulk density were obtained independently on each sample; in general, the values obtained by the GRAPE special 2-minute count are higher and more dispersed than those obtained by the gravimetric methods); and (d) porosity by gravimetric techniques. The porosity varies from 40% to 60% throughout the two holes, depending upon the degree of consolidation of the sediments.

In addition to the individual sampling, wet-bulk density was also determined continuously using the Gamma Ray Attenuation Porosity Evaluator (GRAPE) from Cores 1 to 35 (Hole 548) and from Cores 1 to 7 (Hole 548A). Continuous measurements were stopped when the core diameter became variable or smaller than the diameter of the core liner.

Some shear strength measurements were made using the Torvane. In addition to the standard torsional vane shear with a range 0 to 1 kg/cm^2, we used a sensitive vane adapter with a range of 0.2 kg/cm^2 and a high capacity vane adapter with a range of 2.5 kg/cm^2. Results from physical properties measurements on individual samples are listed in Table 1.

These data allow us to establish correlations between the different physical properties; for example, correlation between the acoustic impedance and seismic reflection profiles (see below).

Correlation of Seismic Profiles with Drilling Results

Detailed multichannel seismic surveys carried out by the Institute of Oceanographic Sciences (U.K.) and several French institutions (Institut Français du Pétrole [IFP]; Centre National pour l'Exploitation des Océans; Comité d'Études Pétroliers Marines) show that a number of buried, tilted blocks bounded by listric normal faults constitute basement beneath the Goban Spur. These blocks trend NW–SE (Montadert et al., 1979) more or less parallel to the continent/ocean boundary. Most of the crests of these tilted blocks are presumed to have been truncated by subaerial erosion during rifting, contributing synrift sediments to the half-graben basins that lie between the blocks. After rifting, during thermal subsidence of the margin, a relatively thin blanket of sediments covered most, although not all, of the rifted blocks and synrift basins.

Site 548 is near the crossing of two multichannel seismic reflection lines—OC 202 (shot point 1340) and CM 18 (shot point (1850). These profiles were acquired using a 48-trace streamer with trace intervals of 50 m. An implosion sound source (Flexichoc) was used for OC 202, and an air gun array was used for CM 18 (shot point intervals of 50 m). Both profiles were processed to obtain a CDP-24-stacked section,[3] but were not migrated prior to drilling. As in all seismic profiles of the industrial type, the frequencies were low (between 10 and 65 Hz). The resultant sound penetration produced a detailed section of the thick synrift deposits but is not favorable for the precise definition of seismic sequences in the relatively thin postrift section (0.5 to 1.5 km.)

The *Glomar Challenger* single-channel seismic profile was shot with two air guns (120 and 105 in.^{3}) while the ship was under way to the site. It achieved shallower penetration but higher resolution than the multichannel system. Nevertheless, detailed seismostratigraphic interpretation is difficult to derive from it because the bubble effect of the source caused repetition of the signal at 150 to 200 ms. This creates a false impression of high resolution and could introduce a large error in the definition of the unconformities separating the seismic sequences. A detailed examination shows several oblique reflectors

[1] Graciansky, P. C. de, and Poag, C. W., et al., *Init. Repts. DSDP*, 80: Washington (U.S. Govt. Printing Office).

[2] Addresses: (Montadert) Institut Français du Pétrole, Rueil Malmaison, France; (Poag) U.S. Geological Survey, Woods Hole, MA.

[3] CDP = constant depth point.

Table 1. Physical properties, Leg 80.

Core-Section (level in cm)	Sub-bottom depth (m)	Sound velocity (km/s)			Bulk density (g/cm^3)		Acoustic impedance $\left(\frac{g}{cm^2/s}\right)10^5$		Porosity (%)	H_2O (%)
			Measurement orientation[a]							
		C°	Parallel	Perpendicular	GRAPE (2 min.)	Wt./vol.	GRAPE	Wt./vol.		
Hole 548										
1-1, 41	0.41	16		1.496						
2-1, 145	5.45	16		1.372	1.659	1.67	2.23	2.29	61.74	37.98
2-3, 134	8.34	16		1.536	1.809	1.71	2.78	2.63	60.41	36.12
2-5, 93	10.93	16		1.531	1.811	1.74	2.77	2.66	58.59	34.41
3-1, 139	14.89	16		1.610	1.857	1.78	2.99	2.87	55.75	32.17
3-3, 142	17.92	16		1.546	1.873	1.79	2.90	2.77	55.46	31.68
3-5, 142	20.92	16		1.532	1.839	1.76	2.82	2.70	56.50	32.95
4-1, 142	24.42	17		1.595	1.833	1.76	2.92	2.81	56.64	32.93
4-3, 135	27.35	17		1.564	1.860	1.82	2.91	2.85	53.67	30.29
4-5, 141	30.41	17		1.538	1.859	1.84	2.86	2.83	53.44	29.76
5-1, 135	33.85	17.2		1.583	1.883	1.84	2.98	2.91	51.82	28.81
5-3, 138	36.88	16.8		1.563	1.797	1.80	2.81	2.81	54.35	30.86
5-5, 114	39.64	16.8		1.565	1.897	1.85	2.97	2.90	52.08	28.88
6-1, 136	43.36	17.5		1.591	1.972	1.78	3.14	2.83	55.60	31.97
6-3, 138	46.38	17.3		1.561		1.77		2.76	55.85	32.31
6-5, 138	49.38	17.6		1.561		1.81		2.83	53.49	30.31
7-2, 24	53.24	19		1.585	1.881	1.84	2.98	2.92	52.03	28.90
7-6, 144	60.44	19.4		1.637		1.82		2.98	52.88	29.76
8-1, 130	62.30	19.3		1.594	1.979	1.79	3.15	2.85	56.35	32.12
8-3, 130	65.30	19.3		1.645	1.965	1.83	3.23	3.01	53.78	30.08
8-6, 130	69.80	19.3		1.624	1.831	1.80	2.97	2.92	55.98	31.91
9-1, 137	71.07	19.3		1.624	1.917	1.83	3.11	2.97	54.32	30.43
10-2, 143	73.43	19.3		1.596	1.997	1.92	3.18	3.06	50.14	26.82
10-4, 136	76.36	19.3		1.643	1.795	1.79	2.94	2.94	56.16	32.10
10-6, 79	78.79	19.3		1.633	1.891	1.87	3.08	3.05	51.60	28.20
11-1, 128	81.28	19.3		1.624	1.920	1.90	3.11	3.08	49.98	26.88
11-3, 124	84.24	19.3		1.650	2.035	2.00	3.36	3.30	45.23	23.19
11-5, 122	87.22	19.3		1.631	1.964	1.91	3.20	3.12	49.99	26.92
13-2, 92	94.42	19		1.594	2.024	1.88	3.23	3.00	52.55	28.61
13-4, 69	97.19	18.8		1.666	1.925	1.88	3.21	3.13	51.19	27.97
13-6, 92	100.42	18.8		1.643	1.943	1.84	3.19	3.02	53.68	29.91
15-2, 119	103.19	18.8		1.641	1.902	1.88	3.12	3.08	51.47	28.11
15-4, 138	106.38	18.8		1.636	1.943	1.92	3.18	3.14	49.09	26.23
15-6, 147	109.47	18.8		1.620	1.950	1.90	3.16	3.08	51.27	27.71
16-1, 123	109.73	20		1.605	1.957	1.90	3.14	3.05	51.27	27.94
16-3, 115	112.65	20		1.618	1.981	1.92	3.21	3.11	49.26	26.23
16-5, 124	115.74	20		1.638	1.937	1.89	3.17	3.10	50.46	27.29
17-1, 130	119.30	20		1.639	2.029	1.95	3.33	3.20	47.79	25.13
17-3, 130	122.30	20		1.680	2.003	1.96	3.37	3.29	46.97	24.58
17-5, 118	125.18	20		1.634	1.919	1.86	3.11	3.04	53.09	29.21
19-1, 137	132.37	19.8		1.621	1.896	1.86	3.07	3.02	52.53	28.87
19-3, 117	135.17	19.8		1.600	1.914	1.89	3.06	3.02	51.19	27.72
20-1, 120	137.20	19.5		1.619	1.994	1.88	3.23	3.04	51.54	28.16
20-3, 120	140.20	19.5		1.611	1.916	1.90	3.09	3.06	49.91	26.97
21-1, 70	141.70	19.4		1.655	1.893	1.92	3/13	3.12	48.32	25.80
21-3, 70	144.70	19.4		1.653	1.950	1.93	3.22	3.20	46.92	24.86
22-1, 121	147.21	19		1.666	1.924	1.92	3.21	3.20	49.38	26.35
22-3, 127	150.27	19		1.666	1.904	1.89	3.17	3.15	50.54	27.32
23-1, 127	152.27	18.9		1.661	1.914	1.91	3.18	3.17	48.72	26.13
23-3, 127	155.27	18.9		1.633		1.89		3.09	50.02	27.14
24-1, 87	156.87	19.4		1.728		1.89		3.27	49.85	27.03
24-3, 87	159.87	19.4		1.679		1.92		3.22	47.36	25.22
25-1, 67	161.67	18.1		1.668	1.868	1.89	3.12	3.15	49.63	26.92
25-3, 67	164.67	18.1		1.676	1.965	1.94	3.29	3.25	46.10	24.31
26-1, 124	167.24	19		1.767	1.904	1.93	3.36	3.41	47.29	25.05
26-3, 124	170.24	19		1.690	1.847	1.94	3.12	3.28	47.36	24.98
27-1, 133	172.33	19		1.667	1.844	1.91	3.07	3.18	49.30	26.41
27-3, 90	174.90	19		1.657	1.961	1.93	3.25	3.20	48.16	25.57
28-1, 100	177	19.2		1.636	1.849	1.91	3.02	3.12	51.97	27.88
28-3, 100	180	19.2		1.680	1.872	1.95	3.14	3.28	48.18	25.29
29-2, 130	183.80	19.2	1.651		1.548	1.92	2.56	3.17	49.93	
30-2, 146	188.96	19.2		1.681	1.722	1.95	2.89	3.28	47.17	24.83
31-2, 148	193.98	19.2		1.687	2.050	1.95	3.46	3.29	49.49	25.95
32-2, 148	198.98	19.2		1.692	1.956	1.96	3.31	3.32	46.63	24.33
33-2, 141	203.91	19.2		1.646	2.003	1.94	3.30	3.19	48.32	25.48
34-2, 147	208.97	19.2		1.681	2.080	1.99	3.50	3.35	46.60	24.03
35-1, 147	210.47	19.9		1.675	2.007	1.97	3.36	3.30	47.39	24.7
Hole 548A										
2-2, 58	207.58	19.9		1.666	1.980	1.92	3.30	3.20	46.27	24.73
2-4, 65	220.15	20.1		1.671	1.926	1.92	3.22	3.21	46.42	24.82
3-2, 147	227.47	20.1		1.691	1.932	1.93	3.27	3.26	45.05	23.86
3-4, 126	230.26	20	1.728	1.725	2.060	1.96	3.55	3.38	44.32	23.19
3-6, 130	233.30	20	1.765	1.748	2.059	1.93	3.60	3.37	45.57	24.21
4-2, 145	236.95	20	1.701	1.696	2.009	1.93	3.41	3.27	46.29	24.60
4-4, 143	239.93	20	1.773	1.627	2.046	1.95	3.33	3.17	46.43	24.45
4-6, 87	242.37	20	1.680	1.695	2.156	1.95	3.65	3.31	46.05	24.20
5-2, 123	246.23	20	1.691	1.770	2.013	1.93	3.56	3.42	45.66	24.30
5-4, 135	249.35	20	1.716	1.722	1.966	1.93	3.38	3.32	45.77	24.27
5-6, 48	251.48	20.6	1.696	1.702	1.914	1.94	3.26	3.30	46.99	24.86
6-2, 114	255.64	20.6	1.708	1.735	2.074	1.97	3.60	3.42	43.49	22.64
6-4, 120	258.70	20	1.778	1.798	1.992	1.98	3.58	3.56	42.33	21.91
7-1, 114	263.64	20.9	1.740	1.737	2.022	1.98	3.51	3.44	42.22	21.85
7-3, 62	266.12	20	1.746	1.740	1.997	1.98	3.43	3.41	42.50	21.95
8-2, 100	274.50	20.4	1.820	1.908	1.868	1.095	3.56	3.72	44.33	23.34
8-4, 83	276.33	20	1.785	1.816	1.984	2.00	3.60	3.63	40.56	20.79
8-6, 93	280.43	20.3	1.887	1.918	1.907	1.92	3.66	3.68	43.48	23.20
9-1, 52	282.02	21.9	1.930	1.989	1.934	1.94	3.85	3.86	41.95	22.15
9-3, 40	284.90	21.3	1.879	1.950	1.979	1.94	3.86	3.78	41.57	22.96
9-5, 37	287.87	21	1.80	1.904	1.973	1.96	3.76	3.73	43.22	22.54
10-2, 87	293.37	21	1.838	1.942	1.466	1.54	2.85	2.99	35.92	23.96
10-4, 81	295.31	21	1.665	1.752	1.964	1.91	3.44	3.35	47.11	25.27
10-6, 87	299.37	21	1.726	1.758	1.887	1.91	3.32	3.36	46.77	25.03
11-1, 74	301.24	20.7	1.789	1.838	1.970	1.90	3.62	3.49	47.88	25.76
11-3, 45	303.95	20.7	1.755	1.760	1.635	2.00	2.88	3.52	41.67	21.33
11-5, 16	306.66	20.6	1.930	2.059	1.827	1.83	3.76	3.77	49.64	27.81

Table 1. (Continued).

Core-Section (level in cm)	Sub-bottom depth (m)	Sound velocity (km/s)			Bulk density (g/cm^3)		Acoustic impedance $\left(\frac{g}{cm^2/s}\right)10^5$		Porosity (%)	H_2O (%)
		C°	Measurement orientation[a] Parallel	Perpendicular	GRAPE (2 min.)	Wt./vol.	GRAPE	Wt./vol.		
Hole 548A (Cont.)										
12-1, 54	310.54	20.6	1.831	1.840	1.941	1.87	3.57	3.44	51.20	28.04
12-3, 58	313.58	20.6	1.950	2.096	1.899	1.83	3.98	3.84	50.69	28.34
12-5, 52	316.52	20.6	1.954	1.896	1.960	1.89	3.72	3.58	49.62	26.94
13-1, 26	319.76	20.6	2.144	2.147	1.258	1.80	2.70	3.86	52.30	29.72
13-3, 11	322.61	20	1.951	2.052	1.029	1.77	2.11	3.63	53.65	31.09
13-5, 17	325.67	20	1.998	2.054	1.922	1.86	3.95	3.82	49.18	27.11
14-1, 68	329.68	20	2.139	2.247	1.851	1.84	4.16	4.13	49.27	27.44
14-3, 63	332.63	20	1.988	2.061	1.861	1.81	3.84	3.73	52.63	29.72
14-5, 27	335.27	20			1.593	1.83			51.38	28.73
15-1, 81	339.31	20	1.306	1.704	1.906	1.82	3.25	3.10	53.35	30.01
15-3, 91	342.41	20	1.661	1.768	1.902	1.78	3.36	3.15	55.76	32.14
15-5, 37	344.87	20	1.713	1.769	1.771	1.17	3.31	3.02	58.97	35.24
16-1, 160	349.60	20	2.811	1.761	1.860	1.73	3.28	3.05	58.02	34.30
16-3, 93	351.93	20	1.746	1.745	1.956	1.80	3.41	3.14	55.41	31.59
17-1, 96	358.46	20	1.732	1.643	1.957	1.81	3.22	2.97	54.22	30.72
17-3, 99	361.49	20	1.794	1.891	1.877	1.83	3.55	3.46	52.21	29.30
17-5, 126	364.76	20	1.691	1.802	1.857	1.78	3.35	3.21	54.69	31.50
18-1, 110	368.10	20.3	2.018	2.023	1.826	1.77	3.69	3.58	55.62	32.28
18-3, 108	371.08	20.3	2.109	2.062	1.908	1.95	3.93	4.02	44.03	23.08
19-1, 75	377.25	20.3	x	1.726	2.234	1.99	3.86	3.43	43.70	22.46
19-3, 102	380.02	20.3	1.975	2.027	2.134	1.98	4.32	4.01	44.62	23.11
19-5, 75	383.25	20.3	1.983	2.049	2.082	2.01	4.27	4.12	42.45	21.69
20-1, 135	387.35	20.3	1.937	1.904	2.108	2.00	4.01	3.81	43.55	22.26
20-3, 110	390.10	20.3	2.044	2.509	1.732	2.05	4.35	5.14	40.64	20.31
21-1, 101	396.51	20.3	2.015	1.971	1.989	1.97	3.92	3.88	43.18	22.48
21-3, 136	399.86	20.3	1.916	1.880	2.122	2.04	3.99	3.85	39.65	19.88
22-1, 28	405.28	20.3	1.961	1.946	2.145	2.04	4.17	3.97	41.85	21.08
22-3, 120	409.20	20.3	2.099	2.070	2.112	2.00	4.37	4.14	43.17	22.10
22-5, 103	412.03	20.3	1.853	1.911	2.304	1.90	4.40	3.63	49.05	26.43
22-7, 19	414.19	20.3	1.715	1.712	2.067	1.93	3.54	3.30	49.25	26.08
23-1, 94	415.44	20.3	1.742	1.723	2.042	1.93	3.52	3.33	49.00	26.00
23-1, 41	417.91	20.3	1.777	1.710	1.971	1.92	3.37	3.28	49.31	26.28
24-1, 10	424.10	20.4	1.753	1.722	2.030	1.91	3.50	3.29	50.62	27.13
24-6, 12	431.62	20.4	1.632	1.688	2.008	1.91	3.39	3.22	49.65	26.61
25-3, 131	437.81	20.4	1.755	1.695	2.007	1.95	3.40	3.31	48.65	25.51
25-6, 30	441.30	20.4	1.764	1.691	1.998	1.95	3.38	3.30	49.43	26.02
26-6, 25	450.75	20.4	1.805	1.757	2.150	1.98	3.78	3.48	46.92	24.30
27-1, 41	452.91	20.4	1.924	1.812	2.139	2.03	3.86	3.68	44.17	22.32
27-3, 72	456.22	20.4	1.960	1.898	2.249	2.12	4.27	4.02	37.59	19.16
27-5, 80	459.30	20.4	1.884	1.855	2.194	2.09	4.07	3.88	39.73	19.50
28-1, 40	462.40	20	1.767	1.836	2.159	2.04	3.96	3.75	43.15	21.70
28-3, 49	465.49	20	1.930	1.854	2.170	2.06	4.02	3.82	41.73	20.73
28-5, 105	469.05	20	1.998	1.623	2.652	1.90	4.30	3.08	48.48	26.20
28-7, 30	471.30	20	1.666	1.894	1.873	1.82	3.55	3.45	52.49	29.62
29-1, 65	472.15	20	1.656	1.642	1.915	1.82	3.14	2.99	53.43	30.04
29-3, 86	475.34	20		1.640	2.475	1.87	4.06	3.07	49.94	27.33
29-5, 80	478.30	20	1.711	1.773	1.465	1.85	2.60	3.28	51.55	28.61
30-1, 141	482.41	20	1.687	1.663	2.158	1.87	3.59	3.11	50.78	27.87
30-3, 48	484.48	20	1.657	1.632	1.953	1.87	3.19	3.05	49.74	27.23
32-2, 58	502.08	20	1.662	1.665	1.928	1.87	3.21	3.11	50.51	27.74
32-4, 39	504.89	20	1.821	1.728	1.959	1.93	3.39	3.34	45.77	24.33
33-1, 113	510.63	20	1.887	2.190	1.669	1.97	3.66	4.31	44.08	22.94
33-3, 95	513.45	20	1.908	1.968	2.061	1.97	4.06	3.88	43.49	22.66
34-1, 120	520.20	20		2.270	1.866	1.88	4.24	4.27	48.51	26.48
34-3, 101	523.01	20	1.920	1.979	1.912	1.87	3.78	3.70	49.64	27.25
34-5, 17	525.17	20	2.383	2.105	2.019	1.99	4.25	4.19	40.81	21.06
35,CC	535.50	20	1.842	1.843	1.861	1.83	3.43	3.37	50.89	28.44
Hole 549A										
1-1, 30	0.80	18.4		1.557	1.808	1.62		2.592	65.36	41.22
1-4, 110	5.60	18.4		1.546	1.384	1.71		2.643	61.12	36.63
2-1, 64	8.64	18.4		1.590	1.917	1.64		2.607	64.31	40.20
2-4, 90	13.40	18.4		1.540	1.866	1.73		2.664	59.91	35.55
3-1, 140	17.64	19.4		1.510	1.818	1.65		2.491	64.41	39.90
3-4, 106	23.06	19.4		1.565	1.785	1.70		2.660	61.02	36.86
4-1, 137	28.37	19.5		1.557	1.790	1.74		2.709	57.89	34.05
4-4, 134	32.84	19.5		1.554	1.683	1.70		2.642	58.70	35.42
5-1, 99	37.49	20		1.561	1.700	1.68		2.622	61.52	37.57
5-4, 90	41.90	20		1.588	1.805	1.71		2.715	59.85	35.9?
6-1, 96	46.96	19.4		1.577	1.791	1.70		2.680	60.29	36.3?
6-4, 96	51.46	19.4		1.551	1.743	1.70		2.636	60.44	36.3?
7-1, 117	56.67	19.4		1.547	1.827	1.69		2.614	60.79	36.87
7-4, 117	61.17	19.4		1.551	1.784	1.71		2.652	59.50	35.61
8-1, 130	66.30	19.6		1.562	1.728	1.68		2.624	60.92	37.06
8-4, 100	70.50	19.6		1.559	1.777	1.72		2.681	59.50	35.50
9-1, 130	75.80	19.6		1.530	1.825	1.67		2.555	61.44	37.4?
9-4, 130	80.30	19.6		1.576	1.733	1.67		2.632	61.44	67.44
10-1, 130	85.30	19.6		1.568		1.66		2.603	61.85	38.13
10-4, 130	89.80	19.6		1.546		1.71		2.643	59.03	35.44
11-1, 135	94.85	18.7		1.557		1.70		2.647	60.16	36.31
11-4, 130	98.30	18.7		1.571		1.69		1.655	60.30	36.48
12-1, 120	104.20	18.7		1.586		1.74		2.759	57.26	33.71
13-1, 120	107.20	18.7		1.540		1.70		2.618	59.81	36.03
14-1, 100	112.00	18.7		1.514		1.67		2.528	61.27	37.63
14-1, 130	112.30	18.7		1.484		1.64		2.433	62.07	38.70
15-1, 110	117.10	18.7		1.525		1.70		2.592	59.91	36.07
17-1, 105	123.55	18.7		1.562		0.75		2.733	56.93	33.38
18-1, 35	125.85	18.7		1.541		1.72		2.650	59.00	35.15
21-1, 15	129.15	18.7		1.561		1.75		2.731	56.37	32.92
24-1, 70	132.70	18.7		1.563		1.79		2.797	53.94	30.85
25-1, 15	135.15	18.7		1.564		1.78		2.784	55.06	31.76
26-1, 90	138.40	18.7		1.554		1.76		1.735	56.06	32.60
27-1, 85	139.35	18.7		1.547		1.75		2.707	57.00	33.34
28-1, 90	140.90	19.7		1.560		1.76		2.745	55.79	32.41
32-1, 130	148.80	19.4		1.585		1.80		2.853	53.99	30.74
33-1, 90	151.40	19.4		1.606		1.80		2.891	53.64	30.48

Table 1. (Continued).

Core-Section (level in cm)	Sub-bottom depth (m)	Sound velocity (km/s)			Bulk density (g/cm³)		Acoustic impedance $\left(\frac{g}{cm^2/s}\right) 10^5$		Porosity (%)	H_2O (%)
			Measurement orientation[a]							
		C°	Parallel	Perpendicular	GRAPE (2 min.)	Wt./vol.	GRAPE	Wt./vol.		
Hole 549A (Cont.)										
34-1, 142	156.92	19.4		1.647		1.81		2.981	53.32	30.15
35-1, 45	160.95	19.4		1.620		1.85		2.997	51.09	28.35
39-1, 135	181.85	19.4		1.585		1.73		2.742	57.24	33.80
40-1, 108	186.58	19.4		1.569		1.79		2.808	54.35	31.10
Hole 549										
2-1, 114	199.64	19.2		1.835	1.874	1.85	3.439	3.395	49.52	27.46
2-3, 119	202.69	19.2		1.879	1.973	1.92	3.707	3.608	45.64	24.32
2-5, 102	205.52	19.2		1.841	1.879	1.85	3.459	3.406	49.61	27.53
3-1, 131	209.31	19.2		1.879	1.909	1.88	3.587	3.533	47.33	25.76
4-1, 30	217.80	19.2		1.821	1.978	1.86	3.602	3.369	49.59	27.33
4-3, 134	221.84	19.2		1.801	1.938	1.85	3.490	3.332	81.14	28.39
4-5, 133	224.83	19.2		1.829	1.936	1.88	3.541	3.439	49.49	26.97
5-1, 85	227.85	19.2		1.886	1.901	1.87	3.585	3.527	48.39	26.50
5-3, 61	230.61	19.2		1.815	1.919	1.89	3.483	3.430	49.27	26.91
5-5, 66	233.66	19.1		1.790	1.896	1.84	3.394	3.294	50.14	27.91
6-1, 53	237.03	19.1		1.803	1.884	1.87	3.397	3.372	49.18	26.98
6-3, 75	240.25	19.1		1.886	1.923	1.87	3.627	3.527	48.85	26.70
6-5, 75	243.25	19.1		1.781	1.913	1.88	3.407	3.348	49.06	26.80
7-1, 51	246.51	19.1		1.915	1.922	1.89	3.681	3.619	47.33	25.70
7-3, 80	249.80	19.1		1.841	2.006	1.93	3.693	3.553	45.86	24.30
7-5, 75	252.75	19.1		1.802	2.028	1.94	3.654	3.496	46.27	24.41
8-1, 109	256.59	19.1		1.890	1.967	1.97	3.718	3.723	44.58	23.22
8-3, 60	259.			1.839	2.058	1.99	3.785	3.650	43.54	22.47
9-1, 17	265.17	19.1		1.942	2.045	2.00	3.971	3.884	41.66	21.31
10-1, 117	275.67	19.2		1.851	2.102	1.98	3.665	3.665	43.80	22.63
10-3, 62	278.12	19.2		1.739	2.141	2.00	3.478	3.478	42.87	21.91
10-6, 75	283.50	19.2		1.901	2.174	2.06	3.916	3.916	40.37	20.06
11-1, 85	284.85	19.2		1.894	2.159	2.04	3.864	3.864	42.33	21.25
11-3, 24	287.24	19.2		1.802	2.044	1.95	3.683	3.514	47.54	24.95
11-5, 75	290.75	19.2		1.812	2.069	1.97	3.749	3.570	46.25	24.06
12-1, 78	294.28	19.6		1.802	2.103	1.99	3.790	3.586	46.58	24.01
12-3, 42	296.92	19.6		1.774	2.123	1.98	3.766	3.513	45.63	23.61
13-1, 85	303.85	19.6		1.936	2.194	2.07	4.248	4.008	39.58	19.55
13-3, 85	309.85	19.6		1.819	2.198	2.01	3.998	3.656	44.05	22.48
13-5, 99	309.99	19.6		1.971	2.176	2.10	4.299	4.139	38.12	18.57
14-1, 89	313.39	19.6		1.984	2.178	2.10	4.321	4.166	38.16	18.62
14-3, 88	316.38	19.6		1.964	2.155	2.09	4.232	4.105	38.19	18.69
14-5, 41	318.91	19.6		1.895	2.177	2.07	4.125	3.923	39.50	19.57
14-7, 10	321.60	19.6		1.769	2.122	1.97	3.754	3.485	47.51	24.73
15-1, 104	323.04	19.5		1.854	2.082	2.00	3.860	3.708	43.96	22.54
15-3, 108	326.08	19.6		2.179	1.686	2.00	3.674	4.358	44.08	22.53
15-5, 94	328.94	19.6		1.862	2.132	2.05	3.970	3.817	40.73	20.31
15-7, 14	331.14	19.6		1.883	2.180	2.07	4.105	3.898	39.81	19.69
16-1, 79	332.29	19.6		1.834	2.167	2.06	3.974	3.778	40.60	20.22
16-4, 82	336.82	19.6		1.900	2.286	2.06	4.343	3.914	40.92	20.34
16-6, 101	340.01	19.6		1.923	2.143	2.01	4.072	3.865	43.61	22.20
17-1, 5	341.05	19.6		1.960	2.152	2.05	4.218	4.018	40.48	20.21
17-3, 90	344.90	19.6		1.746	1.635	1.83	2.855	3.195	52.72	29.52
17-7, 10	350.10	19.6		1.685	1.517	1.58	2.557	2.662	64.90	41.97
17-5, 86	347.86	19.6		1.711	1.590	1.53	2.720	2.618	67.88	45.35
18-1, 121	351.71	19.6		1.720	1.813	1.76	3.118	3.027	57.60	33.44
18-3, 57	354.07	19.6		1.695	1.633	1.62	2.768	2.746	64.25	40.68
19-1, 39	360.39	19.6		1.738	1.679	1.67	2.918	2.902	61.14	37.58
19-3, 12	363.12	19.6		1.899	2.161	2.04	4.104	3.874	41.86	20.98
19-5, 3	366.03					2.05			41.24	20.57
20-1, 27	369.77	19.6		1.907		2.04		3.890	41.43	20.81
20-3, 20	372.70	19.6		1.800		1.99		3.582	44.36	22.83
20-5, 144	376.94	19.6		1.937	2.156	2.09	4.176	4.048	37.32	18.27
21-1, 132	380.32	19.6		2.366	1.783	2.12	4.219	5.016	36.59	17.71
21-3, 130	383.30	19.6		1.892	2.203	2.07	4.168	3.916	39.02	19.33
22-1, 41	388.91	19.6		1.873	2.022	1.98	3.787	3.709	42.40	21.92
22-3, 98	392.48	19.6		1.852	2.480	2.01	4.593	3.723	40.51	20.67
22-5,	394.50	19.6		2.027	2.014	1.90	4.082	3.851	48.00	25.86
23-1, 108	399.08	19.6		2.066	1.991	1.94	4.113	4.008	44.33	23.43
23-3, 131	402.31	19.6		2.314	1.969	1.92	4.556	4.443	45.17	24.08
23-5, 116	405.16	19.6		1.649	2.425	1.97	3.999	3.249	42.61	22.15
24-1, 123	408.73	19.6		1.987	1.934	1.89	3.843	3.755	46.78	25.40
24-3, 123	411.73	19.6		2.130	2.021	1.98	4.305	4.217	41.15	21.31
26-1, 41	426.91	19.6		2.115	2.120	2.05	4.484	4.336	38.18	19.10
27-1, 14	436.14	19.6		1.921	2.215	1.70	4.255	3.266	53.86	32.50
28-1, 116						1.91			44.24	1.91
28-3, 32	448.82	19.6		2.165	1.834	1.84	3.971	3.984	47.66	26.55
29-1, 9	455.09	19.6		2.340	1.960	1.94	4.586	4.540	42.79	22.65
32-1, 13	483.63	19.6		1.784	2.576	1.95	4.603	3.485	43.34	22.72
33,CC	493	19.6		2.871						
34-1, 12	502.62	19.6		2.918	2.152	2.21	6.280	6.449	25.40	11.76
35-1, 27	512.27	19.6		2.295	2.733	2.60	6.272	5.967	7.64	2.60
35-1, 79	512.79	19.6		2.316	1.629	1.99	3.773	4.609	42.98	22.11
39-1, 20	540.70	19.6		1.893	1.913	1.91	3.621	3.616	42.92	22.97
40-1, 29	550.29	19.6		1.951	2.035	2.00	3.902	3.970	42.98	22.07
42-1, 48	568.48	19.6		2.037	2.039	2.03	4.149	4.351	37.21	18.81
42-3, 81	571.81	19.6		1.996	2.073		4.138			
43-1, 41	578.91	19.5		1.954	2.058	2.05	4.021	4.006	35.68	17.82
43-3, 84	582.34	19.5		3.049	2.456	2.40	7.488	7.318	19.09	8.46
44-2, 120	589.70	19.5		2.074	2.049	2.01	4.250	4.169	39.02	19.90
44-4, 41	592.91	19.5		2.009	1.998	2.00	4.018	4.014	39.72	20.34
45-1, 95	598.45	19.5		2.054	2.003	2.61	4.114	5.361	40.42	21.04
45-3, 33	600.83	19.5		2.262	2.153	2.10	4.870	4.750	32.73	15.94
45-5, 46	603.93	19.5		2.012	2.129	1.99	4.284	4.004	40.79	21.02
46-1, 99	607.99	19.5		1.750	2.048	2.01	3.584	3.518	39.17	19.94
46-3, 100	611.	19.5		2.030	1.932	1.93	3.922	3.918	21.11	22.30
47-1, 38	616.88	19.5		2.255	2.384	2.00	5.376	4.510	38.48	19.68
47-1, 52	617.02	19.5		3.229	2.384	2.31	7.698	7.459	23.20	10.30
47-3, 73	620.23	19.5		3.399	2.412	2.38	8.198	8.090	18.60	8.01
47-3, 77	620.27	19.5		2.250	2.074	3.04	4.667	4.590	37.87	18.97

Table 1. (Continued).

Core-Section (level in cm)	Sub-bottom depth (m)	Sound velocity (km/s)			Bulk density (g/cm³)		Acoustic impedance $\left(\frac{g}{cm^2/s}\right) 10^5$		Porosity (%)	H_2O (%)
		C°	Measurement orientation[a] Parallel	Perpendicular	GRAPE (2 min.)	Wt./vol.	GRAPE	Wt./vol.		
Hole 549 (Cont.)										
47-5, 62	623.12	19.5		2.251	2.139	2.07	4.815	4.660	36.23	17.89
47-5, 81	623.31	19.5		3.298	2.387	2.37	7.872	7.816	19.34	8.38
52-1, 31	664.31	19.5		5.460						
52-1, 5	664.05	19.5	?	3.523						
52-1, 31	664.34	20		5.649						
52-1, 50	664.50	20		5.358						
53,CC	673.5	20		2.212	2.468	2.34	5.459	5.176	24.70	10.84
54-1, 136	684.36	19.7		1.955		2.25	4.399		28.79	13.09
54-3, 124	687.24	19.7		1.955	2.388	2.25	4.669	4.399	29.85	13.59
55-1, 89	692.89	19.7		1.783	2.239	2.14	3.992	3.816	35.96	17.18
55-3, 145	696.45	19.7		1.925	2.429	2.25	4.676	4.331	30.38	13.80
55-5, 90	697.40	19.7		1.860	2.411	2.22	4.485	4.129	32.14	14.86
56-1, 35	701.35	19.7		2.017	2.245	2.23	4.528	4.498	31.57	14.50
56-3, 121	705.21	19.7		1.966	2.410	2.25	4.738	4.424	28.77	13.08
56-5, 23	707.23	19.7		2.474	1.919	2.31	4.748	5.715	26.60	11.80
57-1, 108	711.08	19.6		2.049	2.159	2.31	4.424	4.734	26.41	11.71
57-3, 91	713.91	19.6		2.320	2.689	2.37	6.238	5.498	22.18	9.59
57-5, 34	716.34	19.6		1.852	3.084	2.20	5.712	4.074	32.29	15.07
58-1, 79	719.79	19.6		1.846	2.477	2.19	4.573	4.043	31.81	14.86
58-3, 84	722.84	19.6		1.880	2.414	2.22	4.538	4.174	31.18	14.37
58-5, 139	726.39	19.6		1.627	2.302	2.20	3.745	3.579	31.94	14.88
59-1, 126	729.26	19.6		3.095	2.598	2.48	8.041	7.676	15.03	6.20
59-3, 17	731.17	19.6		1.916	2.348	2.22	4.499	4.254	31.01	14.33
60-1, 119	738.19	19.8		2.155	2.440	2.32	5.258	5.000	25.66	11.34
60-3, 50	740.50	19.8		2.629	2.516	2.41	6.615	6.336	20.42	8.69
60-5, 45	743.45	19.8		2.775	2.606	2.42	7.232	6.716	21.17	8.97
61-1, 133	747.33	19.8		1.979	2.283	2.16	4.518	4.275	32.68	15.48
61-3, 80	749.80	19.8		2.105	2.283	2.19	4.806	4.610	30.55	14.20
67-1, no. 5	787.50	20.6		5.385						
67-1, no. 6	787.60	20.6		4.233						
67-1, no. 6	787.60	20.6	4.225							
69-CC, no. 2	793.50	20.6		4.043						
70-1, 56	795.06	20.6		4.065						
71-1, 76	797.76	19.8		3.796						
72-1, 6	801.56	20.6		3.634						
72-1, 70	802.20	20.6		3.451	2.486	2.50	8.579	8.627	13.89	5.69
72-1, 91	802.41	20.6		1.860						
72-2, 133	804.33	20.6		4.219						
73-1, 28	806.78	20.6		1.947	2.514	2.22	4.894	4.322	30.21	13.96
73-1, 40	806.90	20.6		3.594		2.53	9.092		12.36	5.00
73-1, 122	807.72	20.6		3.926						
73-3, 21	809.71	20.6		1.858						
74-1, 73	811.73	20.6		4.149	2.691	2.59	11.165	10.746	7.58	3.00
74-3, 55	814.55	20.6		1.846	2.312	2.19	4.268	4.042	32.45	15.21
74-3, 125	815.25	20.6		4.221	2.759	2.62	11.645	11.059	7.30	2.86
74-3, 129	815.29	20.6		3.143						
75-1, 135	817.35	20.6		4.193	2.688	2.63	11.270	11.027	6.62	2.58
75-3, 34	819.34	20.6		4.181	2.622	2.56	10.962	10.703	9.96	3.99
76-1, 107	826.07	20.5		3.647	2.642	2.56	9.635	9.336	10.13	4.05
76-3, 26	828.26	20.5		3.402	2.602	2.54	8.852	8.641	11.12	4.48
77,CC	834	20.5		3.826						
77,CC	834	20.5		3.984						
78-1, 87	843.87	20		2.940	2.740	2.44	8.055	7.173	17.22	7.24
78-2, 10	844.60	20		1.955	2.119	2.28	4.142	4.457	27.84	12.52
79-1, 58	852.58	20		3.206	2.666	2.53	8.547	8.111	14.22	5.77
80-1, 57	861.57	20		3.963	2.668	2.57	10.501	10.115	8.90	3.55
81-1, 54	865.54	20		2.085	2.002	2.13	4.174	4.441	38.01	18.25
81-2, 34	866.84	20		3.279	2.604	2.53	8.538	8.295	12.33	5.00
82-1, 28	874.78	20		2.750	2.580	2.46	7.095	6.765	17.10	7.11
82-2, 56	876.06	20		1.922	2.543	2.23	4.887	4.286	29.95	13.16
83-1, 96	879.96			1.809	2.406	2.22	4.352	4.016	32.51	15.03
83-2, 110	881.60			2.632	2.749	2.44	7.235	6.422	17.83	7.50
84-1, 127	885.27			1.945	2.465	2.31	4.794	4.493	26.24	11.64
85-1, 16	886.56			4.621	2.845	2.68	13.146	12.384	5.31	2.03
85-2, 9	888.09			1.829	2.383	2.12	4.358	3.877	35.20	17.03
86-2, 131	899.81			1.832	2.479	2.20	4.541	4.030	30.55	14.21
86-3, 8	900.08			3.919	2.700	2.58	10.58	10.111	9.20	3.65
87-1, 133	907.33			1.747	2.510	2.18	4.385	3.808	32.54	15.26
87-3, 30	909.30			3.804	2.76	2.60	10.499	9.89	9.48	3.74
88-1, 93	911.43			3.374	2.703	2.59	9.120	8.738	10.56	4.18
88-2, 50	912.50			1.875	2.447	2.22	4.588	4.162	32.51	14.98
88-3, 62	914.12			2.022	2.403	2.32	4.858	4.691	25.32	11.19
89-1, 93	920.43			4.185	2.714	2.63	11.358	11.006	6.71	2.61
90-2, 58	930.58			2.186	2.458	2.37	5.373	5.180	21.84	9.45
90-2, 114	931.72			2.100	2.431	2.27	5.105	4.767	25.13	11.36
91-1, 27	937.77			1.979	2.457	2.30	4.862	4.551	25.79	11.47
91-2, 56	939.56			2.368	2.214	2.35	5.242	5.564	21.27	10.58
92-1, 64	947.14			2.060	2.413	2.32	4.97	4.779	23.92	9.26
93-1, 68	956.18			4.714	2.835	2.69	13.364	12.680	5.28	2.01
94-1, 24	964.74			4.256	2.625	2.57	11.172	10.938	7.10	2.83
95-1, 22	973.72			4.107	2.556	2.53	10.497	10.390	9.41	3.81
95-1, 68	974.18			4.250	2.624	2.61	11.152	11.092	7.18	2.82
96-1, 37	978.37			4.213	2.627	2.59	11.067	10.911	7.43	2.94
97-1, 53	983.03			4.091	2.623	2.55	10.730	10.432	9.90	3.87
98-1, 106	992.56			3.672	2.522	2.49	9.260	9.143	13.78	5.67
Hole 550										
1-3, 139	4.39	19.5		1.469		1.54		2.262	70.23	46.63
2-1, 23	99.73	19.5		1.534		1.88		2.886	49.80	27.12
3-1, 143	110.43	19.5		1.535	1.841	1.72		2.64	59.56	35.38
4-1, 141	119.91	19.5		1.548	1.842	1.79		2.771	55.74	31.99
5-1, 145	129.45	19.5		1.546	1.882	1.75		2.705	57.58	33.64
5-4, 24	132.74	19.5		1.561	1.920	1.78		2.778	56.11	32.23
6-7, 16	146.66	19.5		1.563	1.984	1.79		2.797	55.29	31.68
7-7, 59	156.5	19.5		1.550	1.921	1.77		2.743	56.20	32.45
8-4, 44	161.44	19.5		1.532	1.848	1.75		2.681	57.23	33.41

Table 1. (Continued).

Core-Section (level in cm)	Sub-bottom depth (m)	Sound velocity (km/s)			Bulk density (g/cm^3)		Acoustic impedance $\left(\frac{g}{cm^2/s}\right) 10^5$		Porosity (%)	H_2O (%)
			Measurement orientation[a]							
		C°	Parallel	Perpendicular	GRAPE (2 min.)	Wt./vol.	GRAPE	Wt./vol.		
Hole 550 (Cont.)										
9,CC (4)	175.4	19.5		1.586	1.856	1.86		2.950	51.12	28.12
11-3, 107	189.07	19.5		1.578	2.788	1.83		2.887	52.20	29.18
12-5, 41	200.91	19.5		1.591	1.934	1.81		2.879	53.65	30.32
14-3, 135	217.85			1.602	2.149	1.92		3.075	48.30	25.83
15-1, 101	224.01			1.652	2.127	1.94		3.205	46.78	24.74
16-1, 118	233.68			1.569	1.990	1.81		2.84	53.96	30.47
17-2, 78	244.28			1.568	2.011	1.85		2.9	52.26	29.02
18-3, 80	255.30			1.616	2.102	1.87		3.022	50.73	27.85
19-1, 88	261.88	19.5		1.615	2.036	1.92		3.100	48.43	25.83
21-2, 52	282.02	19.5		1.642	2.046	1.91		3.136	48.36	25.90
22-1, 87	290.37	19.5		1.653	2.060	1.91		3.157	47.91	25.69
22-4, 66	296.66	19.5		1.684	2.070	1.95		3.283	46.07	24.21
23-2, 61	301.11	19.5		1.690	1.895	1.87		3.16	50.39	27.66
23-5, 43	305.43	19.7		1.699	2.020	1.93		3.279	47.37	25.10
24-2, 103	311.03	19.7		1.622	1.907	1.89		3.065	50.65	27.62
24-5, 102	315.52	19.7		1.622	2.038	1.85		3.0	53.72	29.71
25-1, 72	318.72	19.7		1.706	2.118	1.99		3.39	44.69	23.02
25-6, 58	323.08	19.7		1.626	2.069	1.89		3.073	50.59	27.37
26-1, 26	327.76	19.7		1.653	2.070	1.89		3.124	51.08	27.67
27-1, 26	337.26	19.7		1.696	2.037	1.93		3.273	47.50	25.18
27-5, 73	343.93	19.7		1.726	2.073	1.97		3.4	46.04	24.00
28-1, 135	347.85	19.7		1.730	2.123	2.02		3.494	42.58	21.60
28-4, 96	351.96	19.7		1.765	2.161	2.04		3.6	41.61	20.94
29-1, 116	357.16	19.7		1.759	2.137	2.04		3.588	40.82	20.46
29-4, 96	361.46	19.7		1.725	2.181	2.03		3.501	42.18	21.26
30-1, 34	365.84	19.7		1.803	2.137	2.03		3.66	41.60	20.94
30-4, 106	371.06	19.7		1.820	2.108	2.03		3.694	41.38	20.87
31-1, 143	376.43	19.7		1.712	2.155	2.02		3.458	42.88	21.79
31-3, 82	378.82	19.7		1.770	2.104	2.01		3.557	43.09	21.92
32-1, 141	385.91	19.7		1.739	2.205	2.00		3.478	44.67	22.87
32-6, 98	389.98	19.7		1.841	2.100	1.97		3.626	47.57	24.72
33-1, 42	394.42			1.773	2.081	2.00		3.546	45.50	23.35
33-4, 6	398.56			1.765	2.089	1.99		3.512	45.83	23.62
34-1, 119	404.69			1.766	2.120	1.99		3.514	45.49	23.43
34-4, 123	409.23			1.756	2.054	1.97		3.459	46.17	24.04
35-1, 11	413.11			1.715	1.852	1.84		3.155	50.50	28.02
35-4, 72	418.22			1.607	1.899	1.81		2.908	56.26	31.82
36-4, 14	427.14			1.868	1.947	1.90		3.549	45.67	24.61
37-1, 98	432.98			1.736	2.045	1.96		3.402	45.21	23.63
37-3, 6	435.06			1.812	2.104	1.98		3.587	45.62	23.48
38-3, 110	445.60			1.735	2.032	1.95		3.383	45.24	23.73
38-6, 96	449.94			1.882	2.131	2.05		3.858	40.10	20.08
39-1, 137	452.37	19.7		1.888	2.199	2.08		3.927	38.70	19.09
39-4, 02	455.52	19.7		31.782	2.277	2.08		3.706	38.51	18.99
41-2, 39	471.89	19.7		1.698	2.104	1.99		3.379	43.69	22.46
42-1, 110	480.60	19.7		1.973	2.185	2.09		4.123	38.85	19.08
47-3, 91	525.91	19.7		2.357	2.288	2.25		5.303	28.29	12.88
43-1, 95	489.95	19.7		1.941	2.220	2.15		4.173	35.78	17.07
Hole 550B										
1-1, 94	456.94			1.784	2.257	2.11		3.764	37.93	18.45
1-5, 48	460.48			1.717	2.029	1.97		3.382	46.81	24.36
2-1, 60	466.10			2.182	2.365	2.21		4.822	31.05	14.40
2-3, 27	468.77			1.731	2.080	1.97		3.41	46.08	23.81
3-2, 56	477.06			1.998	2.149	2.08		4.155	38.56	18.98
4-1, 131	485.81			1.850	2.185	2.08		3.848	39.74	19.11
5-1, 18	494.18			1.844	2.273	2.02		3.724	50.13	25.45
5-4, 134	499.84			2.054	2.135	2.07		4.251	39.25	19.47
7-2, 57	515.07			1.967	2.316	2.19		4.307	32.51	15.23
8-1, 45	522.95			2.205	2.273	2.19		4.828	30.66	14.38
8-4, 45	527.45			2.495	2.376	2.29		5.713	24.70	11.07
9-1, 36	532.36			1.926	2.260	2.17		4.179	32.98	15.59
9-4, 58	537.08			1.922	2.227	2.17		4.170	32.48	15.31
10-2, 5	543.50			1.814	2.221	2.12		3.845	36.53	17.64
10-4, 55	546.55			2.176	2.069	2.12		4.613	34.59	16.69
11-1, 48	551.48			2.404	2.458	2.37		5.697	20.91	9.04
11-3, 74	554.74			1.911	2.404	2.11		4.032	37.52	18.25
2-1, 95	561.45	19.7		2.44	2.517	2.40		5.856	19.46	8.29
2-4, 70	565.70	19.7		2.247	2.494	2.27		5.100	26.53	11.96
3-2, 80	572.30	19.7		2.084	2.415	2.25		4.689	28.66	13.03
3-6, 138	578.88	19.7		1.804	2.046	1.99		3.589	44.11	22.74
4-1, 21	579.71	19.7		1.737	1.935	1.93		3.352	47.19	25.09
4-4, 126	585.26	19.7		1.958	2.165	2.11		4.131	35.84	17.43
5-1, 87	589.87	19.7		2.481	2.372	2.30		5.706	23.69	10.55
5-4, 138	594.88			2.224	2.383	2.28		5.070	27.03	12.17
6-1, 41	598.91			2.138	2.336	2.25		4.810	28.32	12.91
17-1, 98	608.98			2.143	2.328	2.23		4.778	28.73	13.19
17-4, 68	613.18			2.008	2.300	2.20		4.417	31.47	14.67
8-1, 68	617.68			1.991	2.315	2.20		4.380	31.58	14.69
8-4, 43	621.93			2.285	2.406	2.29		5.232	26.65	11.93
20-1, 16	635.16			2.114	2.349	2.21		4.671	31.86	14.76
20-4, 12	639.62			2.297	2.466	2.23		5.352	24.07	10.57
21-1, 42	644.42			1.980	2.313	2.19		4.336	32.33	15.16
21-6, 38	648.88			1.995	2.273	2.19		4.369	32.06	15.02
22-1, 104	654.04			2.030	2.322	2.33		4.525	29.98	13.74
22-4, 83	658.33			1.940	2.286	2.19		4.248	32.69	15.33
23-1, 17	662.17			1.974	2.266	2.18		4.303	32.91	15.48
23-4, 1	666.51			1.842	2.036	2.09		3.849	38.26	18.73
24-1, 142	672.42			2.047	1.797	2.15		4.401	34.64	16.47
25-2, 27	681.77			1.909	2.265	2.16			36.27	16.25
25-4, 04	684.54		4.940		2.634					
26-2, 6			4.281		2.627					
26-3, 9			5.382		2.857					
27-1, no. 1B			4.707							
27-1, no. 3B			4.195							
27-1, no. 3B			4.361							

Table 1. (Continued).

Core-Section (level in cm)	Sub-bottom depth (m)	Sound velocity (km/s) C°	Measurement orientation[a] Parallel	Perpendicular	Bulk density (g/cm³) GRAPE (2 min.)	Wt./vol.	Acoustic impedance $\left(\frac{g}{cm^2/s}\right) 10^5$ GRAPE	Wt./vol.	Porosity (%)	H_2O (%)
Hole 550B (Cont.)										
27-2, no. 3A			4.201							
27-2, no. 3A			4.031							
27-3, no. 2D			3.819		2.572					
27-3, no. 2E			4.317							
28-1, no. 2E			4.036		2.535					
27-1, 5			3.926		2.511					
28-4, no. 1B			5.501		2.875					
28-4, no. 1B			5.505							
28-4, no. 1B			5.212							
29-2, no. 1C			4.020		2.634					
29-5, no. 1F			5.579		2.894					
30-1, no. 1E			4.958		2.758					
30-2, 42			4.540		2.727					
30-4, 4D			5.470		2.841					
30-4, 115			5.525		2.812					
Hole 551										
H2-1, 143	95.93			1.560	1.835	1.73			58.06	34.45
H2-3, 143	98.93			1.544	1.790	1.73			57.19	33.92
H2-5, 116	101.66				1.838	1.77			54.64	31.61
2-2, 124	106.74			1.592		1.78			55.59	31.97
3-3, 145	117.95			1.633	1.923	1.84			51.55	28.66
4-1, 142	124.42			1.760	1.895	1.87			49.59	27.16
4-3, 25	126.25				1.394	1.86			50.09	27.65
4,CC (4)	127.54			1.616	1.953	1.89			49.15	26.70
5-1, 141	133.91			1.626	1.946	1.85			51.49	28.57
6-1, 147	139.97			1.949	1.917	1.82			48.21	26.34
6-3, 40	141.90			1.975	2.131	2.08			36.85	18.19
6-4, no. 1A	163.12			4.600						
6-4, no. 1B	143.27		4.578							
6-4, no. 1C	143.50		4.605		2.216					
6-4, no. 1C	143.50		4.548							
6-4, no. 1C	143.51		4.890							
8-1, 5-7			5.085		2.260					
9-1, 49			4.629		2.676					
9-4, 19			4.833		3.058					
10-2, 81			5.109		2.749					
11-1, 18			5.257		2.764					
11-5, 29			4.570		2.722					
11-7, 84			4.929		2.700					
12-2, 7			5.476		3.814					
12-5, 6			4.487		2.803					
12-4, 72			4.462		2.715					
13-1, 42			4.472		2.676					
13-5, 63			4.699		2.825					
13-5, 152			3.983		2.703					
14-1, 58			4.849		2.720					
14-1, 129			4.853		2.754					

[a] With respect to bedding.

crossing more horizontal reflectors, the oblique ones being misleading repetitions of the signal. As a result of these complications, the correlation of the seismic lines with the results of the drilling is only tentative.

Steps for Correlating Seismic Profiles with Drilling Results

The first step is to identify depositional sequences (i.e., stratigraphic units composed of a relatively conformable succession of genetically related strata; Vail et al., 1977). The sequences can be easily defined when their boundaries are unconformities as shown by lateral terminations that meet adjacent reflectors at an angle (termed onlap, downlap, toplap, and truncation).

The boundaries of depositional sequences are usually, but not always, high-amplitude reflectors (if lithologies are similar in successive sequences, they are not). The identification of the boundaries of depositional sequences on seismic reflection profiles allows a first-order correlation with Holes 548 and 548A, because in most cases these boundaries correspond to unconformities defined by biostratigraphic and lithostratigraphic analysis.

Because a seismic reflection depends on the acoustic impedance contrast between adjacent strata (i.e., the product of the compressional sound velocity and the wet-bulk density), the best way to correlate a DSDP hole with a seismic reflection profile would be to generate a synthetic seismogram from the sonic velocity and density logs. This synthetic seismogram could then be compared with the seismic reflection profile. However, since this cannot be achieved on board *Glomar Challenger*, the second step is to determine (from physical properties measured on shipboard and from downhole logging) what interfaces in the holes can cause the major reflections. Then one uses sonic velocities to calculate the sonic travel time required to reach the different reflectors.

Site 548 Depositional Sequences

The geological framework of the area is shown by the multichannel profiles (Fig. 1 and Poag et al., this vol.). The site is located on a tilted block, the crest of which has been truncated by a conspicuous horizontal erosional surface. To the southwest the block is bound by a listric normal fault that delineates a half graben filled with synrift and postrift sediments. To the northeast of the block, the upper boundary of a sequence of inclined synrift beds forms an important unconformity that is continuous with the erosional surface that truncates the

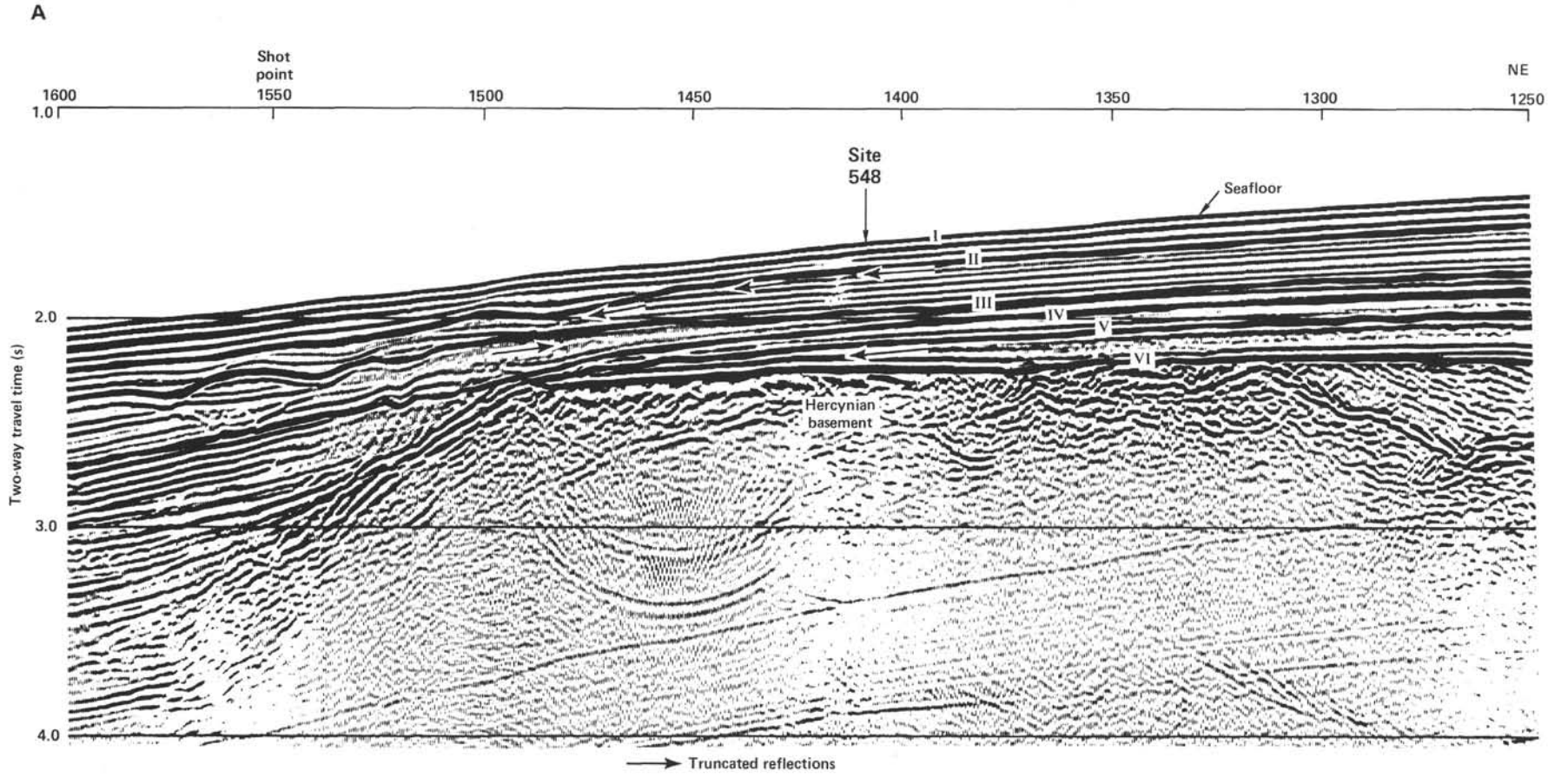
A
Shot point
1600
1550
1500
1450
1400
1350
1300
1250
NE
1.0
2.0
3.0
4.0
Two-way travel time (s)
Site 548
Seafloor
I
II
III
IV
V
VI
Hercynian basement
Truncated reflections

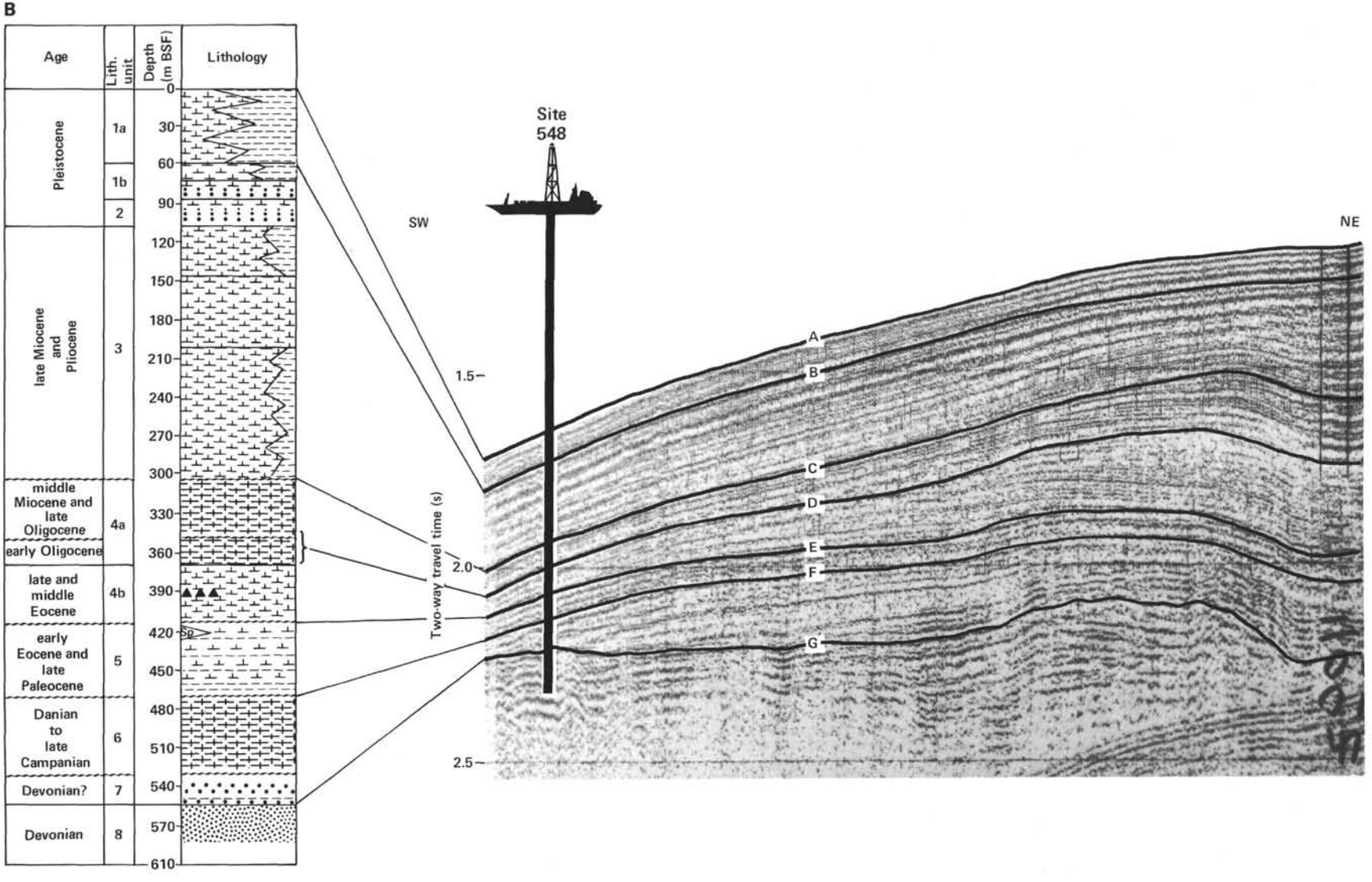

Figure 1. Depositional units near Site 548. A. Major unconformities on line OC 202 as it crosses near Site 548. B. Major reflectors on *Glomar Challenger* seismic line crossing Site 548. Correlation of seismic reflectors with drilled stratigraphy shown in left-hand column. Symbols used for lithology as defined in Explanatory Notes (this vol.).

basement block. Above this unconformity there is a sequence of subhorizontal postrift sediments that displays variable reflections. The thickness of the postrift sediments varies from 520 ms to 660 ms (two-way travel time) on top of the basement block.

Northeast of Site 548 on line OC 202, several sequence boundaries can be identified by downlap, onlap, or toplap of reflections. Extension of these sequences to Site 548 is difficult and imprecise because of the thinness of the section and the low frequencies used to produce the seismic profiles. Moreover, Site 548 is located 2 km away from seismic profile OC 202. Nevertheless, we recognize the following boundaries at shot point 1435 on line OC 202 (see Fig. 1A), where the thickness of the sediments is the same as that on the *Glomar Challenger* profile, which does cross the site.

Boundary	Feature	Two-way travel time, ms (or ms BSL)
I	Seafloor	1640
II	Unconformity	1760 (or 120 [or less])
III	Unconformity	1920 (or 280)
IV	Unconformity	2040 (or 400)
V	Unconformity	2120 (or 480)
VI	Basement	2220 (or 550)

Distinct seismic sequences are evident on the *Glomar Challenger* profile, but their exact boundaries are difficult to determine because of the bubble effect. Figure 1B shows the boundaries that can be identified:

Boundary	Feature	Two-way travel time, ms (or ms BSL)
A	Seafloor	1680
B	Unconformity	1750 (or 70)
C	Unconformity (important)	1950 (or 270)
D	Unconformity (not clear)	2050 (or 370)
E	Unconformity (important)	2125 (or 445)
F	Unconformity (not clear)	2160 (or 480)
G	Basement	2225 (or 545)

Correlation of *Glomar Challenger* Profile and Multichannel Profiles

The following table shows the correlation between the unit boundaries defined on the *Glomar Challenger* profile and the multichannel profiles. The correlation is tentative, because the frequencies used are different and the scales of the sections are different. However, there is a good first-order correspondence between the boundaries defined on both profiles.

OC 202 profile boundary	Two-way travel time (ms)	*Challenger* profile boundary	Two-way travel time (ms)
I (seafloor)	0	A	0
II	120 (or less)	B	70
III	280	C	270
IV	400	D	370
		E	445
V	480	F	480
VI	550	G	545

Relationship between Seafloor Depth and Two-Way Travel Time at Site 548

Excellent correlations exist between the lithologic units of Hole 548A and the downhole logs. The sonic log records the transit time per unit length, but by integration, the thickness of formation equivalent to 1 or 10 ms of one-way travel time can be derived. Thus, theoretically one can directly establish the travel time–depth relationship. However, the top and the bottom of Hole 548A were not logged, and cycle skipping at different levels has complicated the interpretation.

We have additional data from the shipboard physical properties measurements (i.e., sonic velocity perpendicular to bedding, or density); thus, the acoustic impedance can be calculated. Velocities and densities are plotted versus the lithologic units in Figure 2.

The validity of this simple processing of the data is corroborated by the good accordance between the total travel time to basement calculated from velocity measurements (558 to 559 ms) and the travel time measured on the seismic profiles (550 ms). Nevertheless, it is evident that all the boundaries of intervals chosen for the calculations cannot generate reflections visible on our profiles. The intervals are often too thin to be resolved by the low frequencies used in this type of seismic profiling (an interval must be several tens of meters thick to be resolved). The final interpretation for the correlation of Site 548 with the seismic profiles is given in Figures 3 and 4. The seismic boundaries correlate with sharp changes in lithology marked by unconformities (e.g., Eocene marls on lower Paleocene chalks, or the cherty middle Eocene on the lower Eocene marls) and with pronounced changes in acoustic impedance between conformable sequences (as at the base of the upper Miocene).

Figure 1B shows the proposed correlation between the *Glomar Challenger* profile and the different lithologic units and unconformities at Site 548.

SITE 549

Physical Properties

Measurements Made

At Site 549 four physical properties (sound velocity, wet-bulk density with the GRAPE special 2-min. count, wet-bulk density, and porosity) were measured on undisturbed samples taken every two sections (when the recovery was good). When the recovery was poor, we tried to make one or two measurements per core. Nevertheless, in some intervals we were not able to make any measurements.

In some sections, like the Lower Cretaceous sandy dolosparite and the basement, we took several velocity measurements. The GRAPE was not run in the continuous mode on Hole 549 cores. In Hole 549A, we measured sound velocity, wet-bulk density, and porosity on samples taken every three sections.

A record of the GRAPE special 2-minute count was made only from Cores 1 to 9, where continuous GRAPE could not be run (the recorder failed). The results are

compiled in Table 1 and plotted in Figure 5 at the same scale as used for the stratigraphic log and downhole logs. Fifty-five shear strength measurements were made using the Torvane. Shear strength in kg/cm^2 is listed in Table 2.

Discussion

The physical properties of the Site 549 cores display large variations in response to variable lithification and lithology. The velocities measured on the samples correspond closely to the velocities measured by the sonic log. This correspondence permitted the determination of interval velocities, which were used for correlating the borehole lithologies with the seismic profiles.

Lithologic Unit 1 is characterized by low velocities (1.52–1.55 km/s) and high porosities (between 60 and 65%), with variations reflecting alternating marly calcareous and foraminifer–nannofossil oozes.

Lithologic Unit 2 (nannofossil oozes and chalks) can be subdivided on the basis of physical properties. There is a clear break near 130 m (near the Oligocene/Eocene boundary). Above this break, velocities are consistently low (1.55 km/s) and porosities are high (60%); below the break, velocity increases to 1.7 to 1.8 km/s at about 200 m, from which point it stays constant. The porosity curve shows a similar pattern (values drop to 50%).

Lithologic Unit 3 (marly chalks and chalks) has a mean velocity of 1.9 km/s and a mean porosity of 40 to 45%. A bed in Subunit 3-d containing radiolarian- and diatom-rich nannofossil chalk is particularly noticeable on the log by its low velocity (1.6 km/s), low density (1.6 g/cm^3), and high porosity (60–65%).

Lithologic Units 4 and 5 (nannofossil chalks) are characterized by an increase of the mean velocity (2.45 km/s) and decrease of porosity (40%). The silty calcareous mudstones of Unit 4 can be subdivided into two subunits on the basis of the physical properties and downhole logs. From 478 to 631 m, the mean velocity is around 2.1 km/s (some values are as high as 3 km/s); from 631 to 661 m (no recovery), velocity attains 2.5 km/s.

The sandy dolosparite of lithologic Unit 7 displays the highest velocity of any section at this site (5.5 km/s).

Unit 8 has a mean velocity of 2.5 km/s and a porosity between 20% and 30%. The calcarenite of Unit 9 has a mean velocity of 3.4 km/s.

Lithologic Unit 10 is characterized by alternations of mudstones, sandstones and wackestones having velocities of 2 to 4.5 km/s.

The sandstones of the Hercynian basement have a relatively low velocity (about 4.2 km/s), which may explain the lack of a distinct reflector at the base of the synrift deposits (Units 8 to 10) near the site.

The shear strength measured on cores from Hole 549A varies from 0.150 kg/cm^2 in the Pleistocene to 1 kg/cm^2 at 150 m depth in the upper Eocene. Piston coring became increasingly difficult near 120 to 130 m depth, and recovery was poor below 160 m. This could be linked to the change of physical properties and increase in shear strength at about that depth.

Correlation of Seismic Profiles with Drilling Results

IFP profile OC 507, parallel to the Pendragon Escarpment, crosses profile CM 10 near the crest of the adjacent basement block. Site 549 was located north of shot point 2200 on CM 10. The point of profile CM 10, which is at an equivalent water depth and appears to be on strike with Site 549, is close to shot point 2533 and is used for establishing correlations with the drilled section.

The same method used at Site 548 was used for the correlation of the seismic profile and the results from Holes 549 and 549A.

Definition of Seismic Sequences

The migrated section CM 10 (scale of 10 cm/s) displays the following seismic sequences near Site 549 (Fig. 6).

Sequence A. Not clearly defined on the profiles because of the strong bottom reflector. Inferred from lithologic data, which show a thin Pleistocene veneer.

Sequence B. Relatively transparent sequence; less transparent updip. Onlaps Sequence C slightly and is thin at the site. Affected by a series of normal faults.

Sequence C. Characterized by a peculiar seismic facies all along profile CM 10; exhibits a series of strong discontinuous reflectors, which appear to have been cut by a series of closely spaced normal faults. Basal reflector truncates underlying sequence, especially near the site. Sequence nearly pinches out updip on the next truncated basement high.

Sequence D. Weak reflectors; thin under Site 549; thickens updip before it pinches out.

Sequence E. Characterized by weak reflectors; progrades downdip, downlapping the underlying sequence, except under Site 549, where it onlaps a depositional high. Also pinches out updip and seems to have been affected by a small, normal fault at shot point 2550. Only upper part of sequence represented at Site 549.

Sequence F. Transparent; fills broad depression, pinches out updip on Sequence G. Downdip, appears to crop out along Pendragon Escarpment. Locally onlaps depositional high near Site 549; therefore, lower part of sequence is missing at the site. Base of Sequence F is well delineated by a strong reflector. Geometry of sequence and absence of faulting demonstrate that deposition of Sequence F postdates rifting of margin.

Sequence G. Characterized by series of strong reflectors that apparently prograde downdip, downlapping underlying sequence and pinching out completely before reaching Site 549. Updip the sequence seems to abut against next basement block. The wedge-shaped cross sectional geometry of Sequence G suggests synrift accumulation.

Sequence H. Typical synrift depositional sequence, except near the site, where it locally thickens. Prominent wedge-shaped geometry reflects deposition during tilting of the block. Seems to abut against next block. Base marked by strong reflector interpreted as top of Hercynian basement. Near the site, the sequence thickens, resembling a reefal buildup or a large dune.

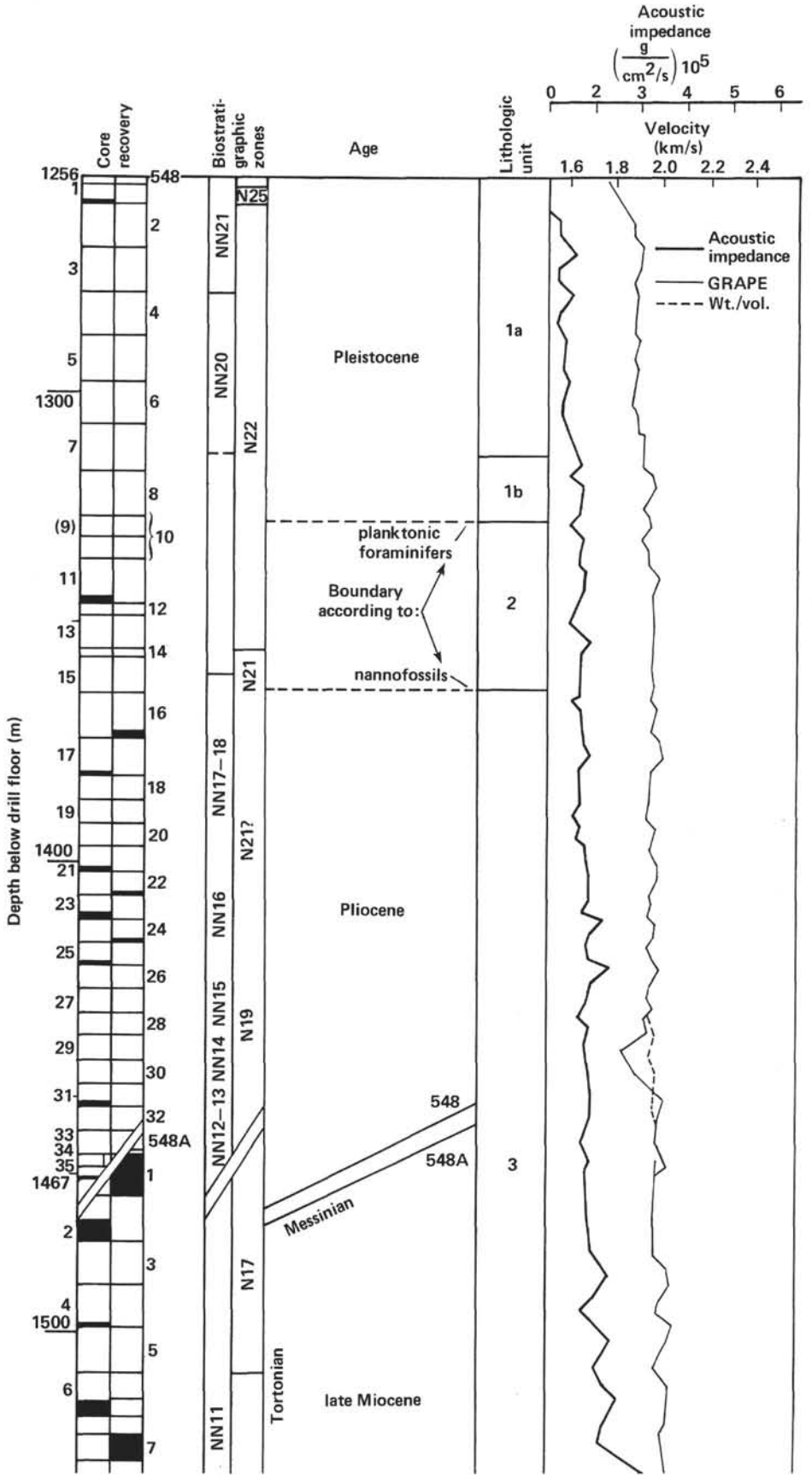

Figure 2. Correlation of stratigraphy with physical properties, Site 548.

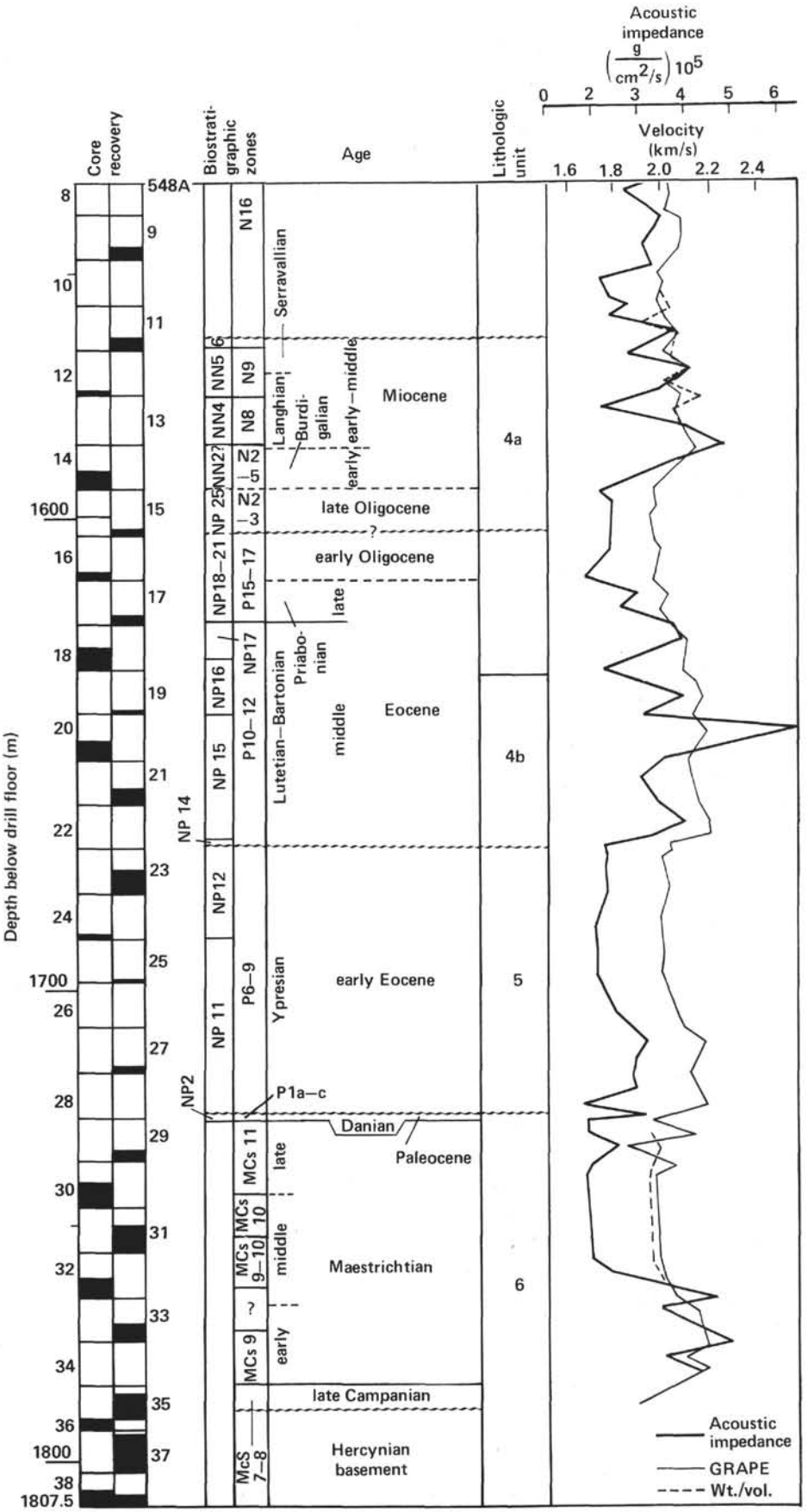

Figure 2. (Continued).

Boundary depth (m)	Interval velocity (m/s)	One-way travel time per interval (ms)	Cumulative two-way travel time		Stratigraphic level of sequence boundaries	Sequence boundaries on seismic profile
			as measured (ms)	corrected for pressure (-5%)		
0					Seafloor	I, A
	1560 ± 50	38.5				
60			77	73	Intra-Pleistocene	II, B
	1660 ± 60	100.6				
227			278	264	top upper Miocene	
	1805 ± 60	15.5				
255			309	294		
	1830 ± 85	14.7				
282			338	321	base upper Miocene	III, C
	1960 ± 120	14.7				
335			368	350	base Miocene	
	1790 ± 80	19.5				IV, D
370			407	387	top middle Eocene	
	1980 ± 120	22.7				
415			453	430	middle/lower Eocene	E
	1700 ± 15	20.6				
450			494	469	intra–lower Eocene	
	1800 ± 90	13.8				
475			522	500	lower Eocene/lower Paleocene	V, F
	1680 ± 50	20.8				
510			563	535	Intra–Upper Cretaceous	
	2060 ± 120	12.1				
535			588	559	Basement	VI, G

Figure 3. Depth and age of sequence boundaries, Site 548.

At Site 549 (CM 10), the two-way travel times from the seafloor to the boundaries of the seismic sequences visible in the area of shot point 2533 are:

Boundary at shot point 2533	Two-way travel time at Site 549 (ms)	Remarks
1	0	Seafloor.
2	—	Not visible at Site 549.
3	90	Travel time not precise.
4	370	
5	460	
6	535	
7	—	Not present at Site 549.
8	690	
9	960	Not conspicuous. Basement.

Near the site, the boundaries of the seismic sequences are strong reflectors and must therefore correspond in the hole to changes in physical properties.

Depth–Travel Time Relationships at Site 549

We calculated acoustic travel time after determining mean velocities for selected intervals between unconformities and changes in acoustic impedance. The velocities are imprecise because recovery was poor and the sonic log was affected by repeated cycle skipping. For Sequence A we used the same velocities as at Site 548. For the older sequences we used mainly the values obtained from the sonic log.

The values are presented on Figure 7. Depth versus two-way travel time is shown in Figure 8. Even though Site 549 was not exactly on profile CM 10 and the velocities are not precise, the calculated positions of boundaries appear to fit the seismic sequences well.

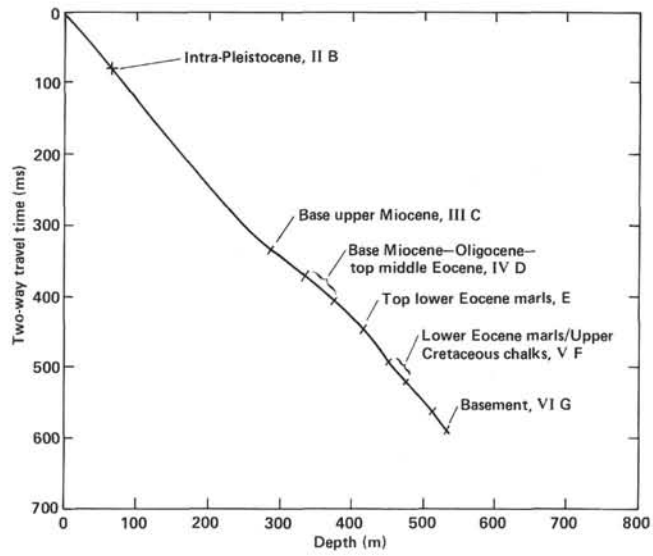

Figure 4. Two-way travel time versus depth, Site 548.

Correlation

The following correlations of seismic profile CM 10 can be made with the stratigraphy of Site 549 (Fig. 9).

Sequences A, B and C represent the Pleistocene, Pliocene (absent at the site), Miocene (reduced at the site), Oligocene and the upper-middle and parts of the lower Eocene (lithologic Units 1 and 2). The boundary between Sequences B and C cannot be picked precisely near the site, but it may correspond to the late Oligocene disconformity near 95 m BSF. The base of Sequence C is an unconformity within the lower Eocene but was not recognized by biostratigraphy. It seems to correspond more or less to the top of lithologic Unit 3 (marked by

Table 2. Shear strength, Hole 549A.

Core	Section	Depth from top of section (cm)	Shear strength (kg/cm^2)
2	1	1.25	0.150
	2	1.20	0.110
	3	1.20	0.154
	4	1.20	0.170
	5	1.20	0.175
	6	1.20	
	7	1.20	0.180
5	1	1.40	0.290
	2	1.40	0.320
	3	1.40	0.350
	4	1.40	0.380
	5	1.20	0.345
	6	1.40	0.600
6	1	1.40	0.320
	2	1.40	0.380
	3	1.40	0.245
	4	1.40	0.175
	5	1.40	0.220
	6	1.40	0.250
7	1	1.40	0.320
	2	1.40	0.370
	3	1.40	0.340
	4	1.40	0.380
	5	1.40	0.370
	6	1.40	2.75
8	1	1.40	0.400
	2	1.40	0.340
	3	1.40	0.365
	4	1.40	0.365
	5	1.45	0.420
	6	0.60	0.430
9	1	1.40	0.470
	2	1.40	0.540
	3	1.40	0.810
	4	1.40	0.670
	5	1.30	0.600
10	1	1.40	0.350
	2	1.40	0.350
	3	1.40	0.450
	4	1.40	0.412
	5	1.40	0.450
	6	1.40	0.625
11	1	1.40	0.425
	2	1.40	0.575
	3	1.40	0.475
	4	1.40	0.537
	5	1.40	0.825
	6	1.40	0.550
14	1	1.40	0.500
	2	0.05	0.550
27	1	0.77	0.475
	1	1.05	0.400
28	1	1.40	0.525
33	1	1.40	0.812
	2	1.40	0.987
34	1	1.40	1.050

the increase in clays and the sharp increase in the intensity of NRM in NP14).

Sequence D comprises the lower Eocene and upper Paleocene marly chalks of lithologic Unit 3.

Sequence E represents the Upper Cretaceous chalks of lithologic Units 4 and 5 (bounded above and below by unconformities).

Sequence F corresponds to the middle and lower Albian mudstones of lithologic Unit 6. This sequence seems to be the oldest postrift unit at the site.

Sequence H represents the very shallow water synrift deposits of lithologic Units 7 to 10 of Barremian–Hauterivian(?) age resting on the Paleozoic basement.

Sequence G is not present at the site; it probably also corresponds to synrift deposits of late Barremian to Aptian or earliest Albian age. The exact age of the breakup unconformity thus cannot be determined very accurately, but if this interpretation is correct it should be pre–early Albian in age, or at least intra–early Albian.

SITE 550

Physical Properties

Measurements Made

At Site 550 we measured three physical properties on samples taken every three sections (sound velocity with the Hamilton Frame perpendicular to bedding; wet-bulk density with the GRAPE special 2-min. count; wet-bulk density–water content–porosity by gravimetric techniques) (Table 1 and Fig. 10).

Sound velocity of basalts was measured on half-cores and plugs. Gravimetric techniques were not used on these plugs in order to keep them saturated for later onshore conductivity measurements. A GRAPE special 2-minute count was made but without introducing a grain density in the calculation to obtain true wet-bulk density. In addition to the individual sampling, wet-bulk density was also determined continuously (Core 1 to Core 37 in Hole 550) using the GRAPE.

Discussion

At Site 550 we used mainly the downhole logs to establish correlations between the seismic profile and the drilled section. Physical properties measured on board ship display the same broad changes as the logs, but important differences between some absolute values have been noted and must be more thoroughly studied onshore. For example, velocities measured on samples are systematically 15 to 20% lower than velocities obtained by downhole logs, but density and porosity values measured on samples and by logging are comparable. A relatively sharp drop in porosity values takes place between about 450 m BSF and about 510 m BSF (values of 40–45% to about 30%). This occurs in the upper part of the Maestrichtian turbidites and is probably linked to a certain stage of compaction.

Mean velocities of the different lithologic units encountered in the holes are presented in the next section. Velocities of basalts varied from 3.8 to 5.5 km/s.

Correlation of Seismic Profiles with Drilling Results

Site 550 was drilled 10 km southwest of the supposed ocean/continent boundary (Fig. 11). The seismic profiles display vividly (Fig. 12) buried topographic highs and lows of the oceanic crust generally covered by about 1 km of sediments. The tectonic style of the oceanic crust is characterized by asymmetric faulted blocks that are tilted toward the margin as typically present on the flanks of mid-oceanic rift systems. Some coherent reflectors that exist within the oceanic crust probably correspond to lava flows.

Site 550 was spudded on top of one of the basement highs in order to minimize the penetration required and

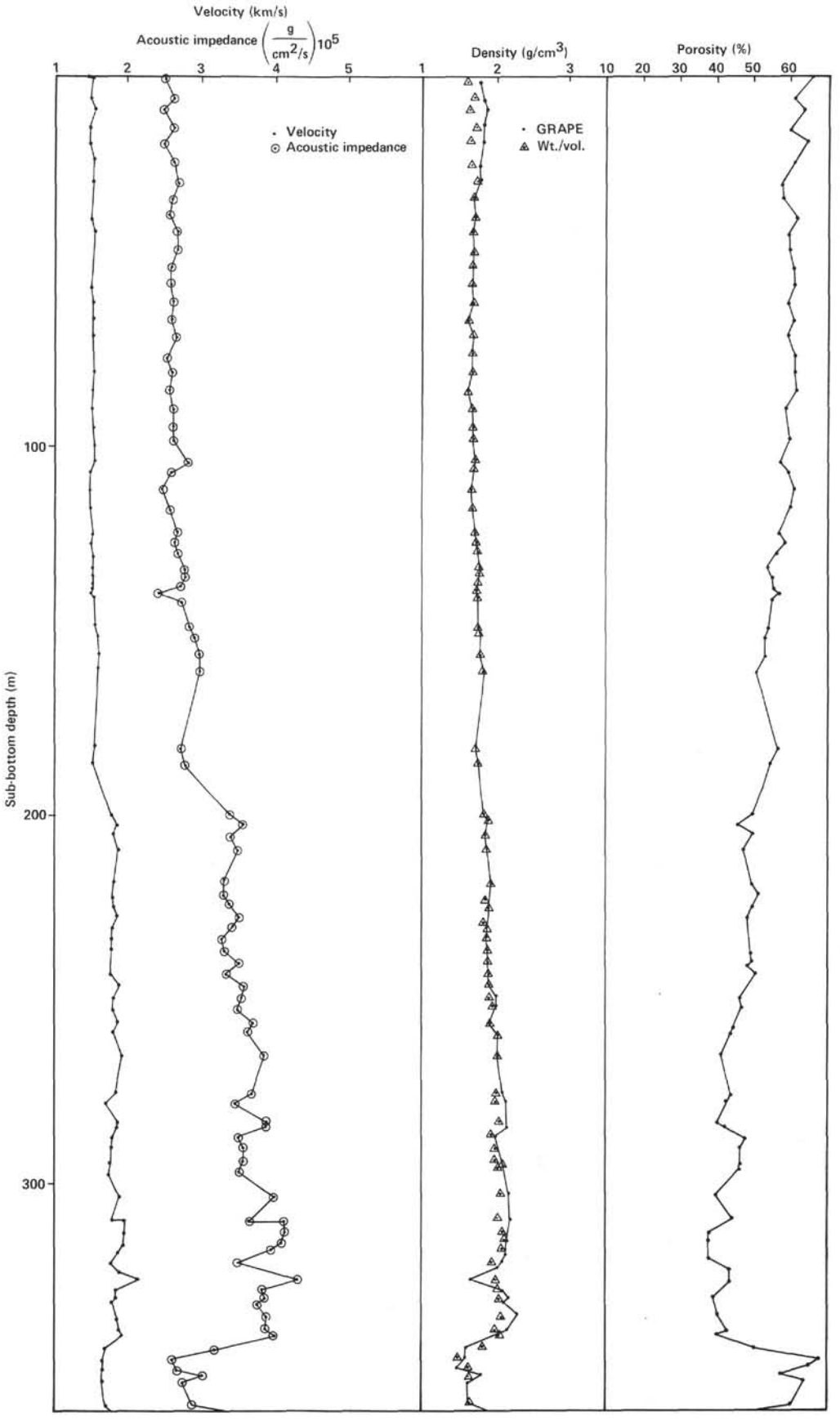

Figure 5. Physical properties, Site 549.

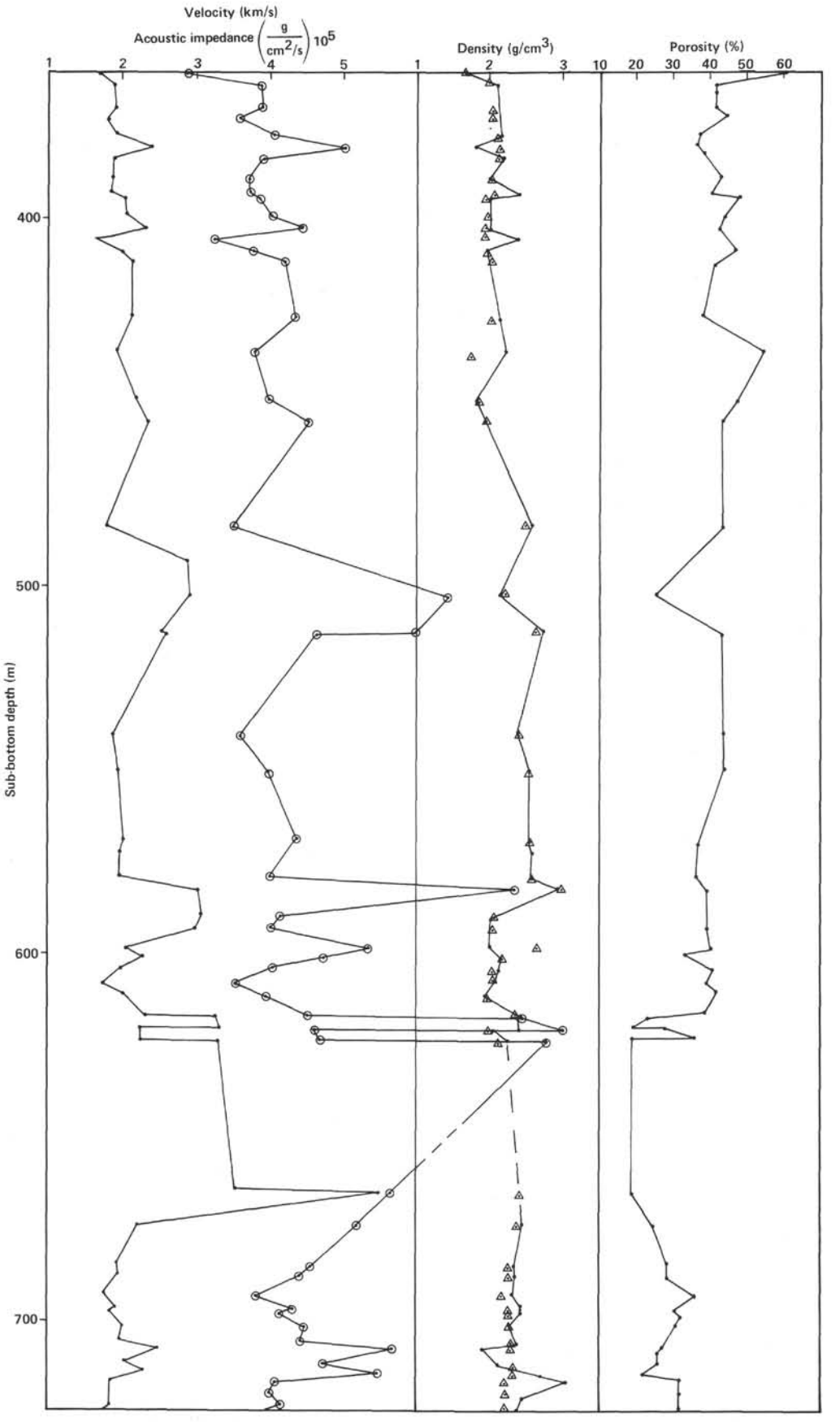

Figure 5. (Continued).

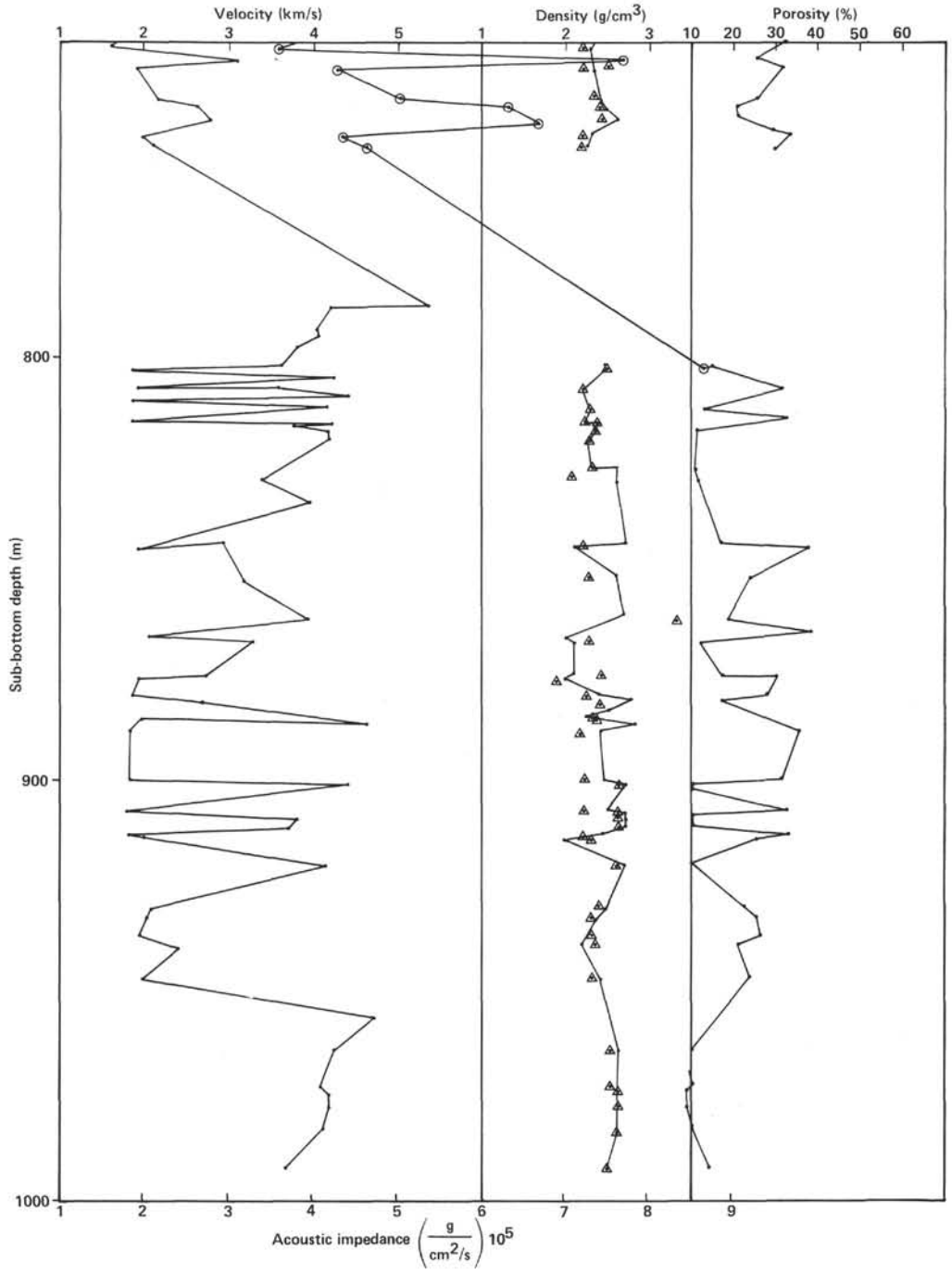

Figure 5. (Continued).

because the profile shows that the oldest layers in the depressions seem to drape over the high and thus would be cored.

Along profile IOS CM 11, three main seismic sequences can be traced widely and can also be identified beneath Site 550 (Figs. 11 and 12). These sequences, from bottom to top, have the following general characteristics:

Sequence C is characteristically almost transparent. It has faint discontinuous reflectors, except for one strong reflector that is often present at its base just above the oceanic crust. This sequence has filled many basement lows but does not cover the tops of all the major blocks. Its thickness varies from 0 to 300 ms. Its arching reflectors frequently are truncated by the overlying sequence, as at Site 550.

Sequence B is characterized by a series of strong continuous reflectors. Its thickness varies from 0 to 300 ms (reflecting the topographic undulations of the underlying sequence). Its upper reflections are truncated by the overlying sequence. The majority of the small compaction faults present over basement highs cannot be traced above the upper boundary of Sequence B.

Sequence A is approximately 300 ms thick and is characterized by discontinuous faint reflectors.

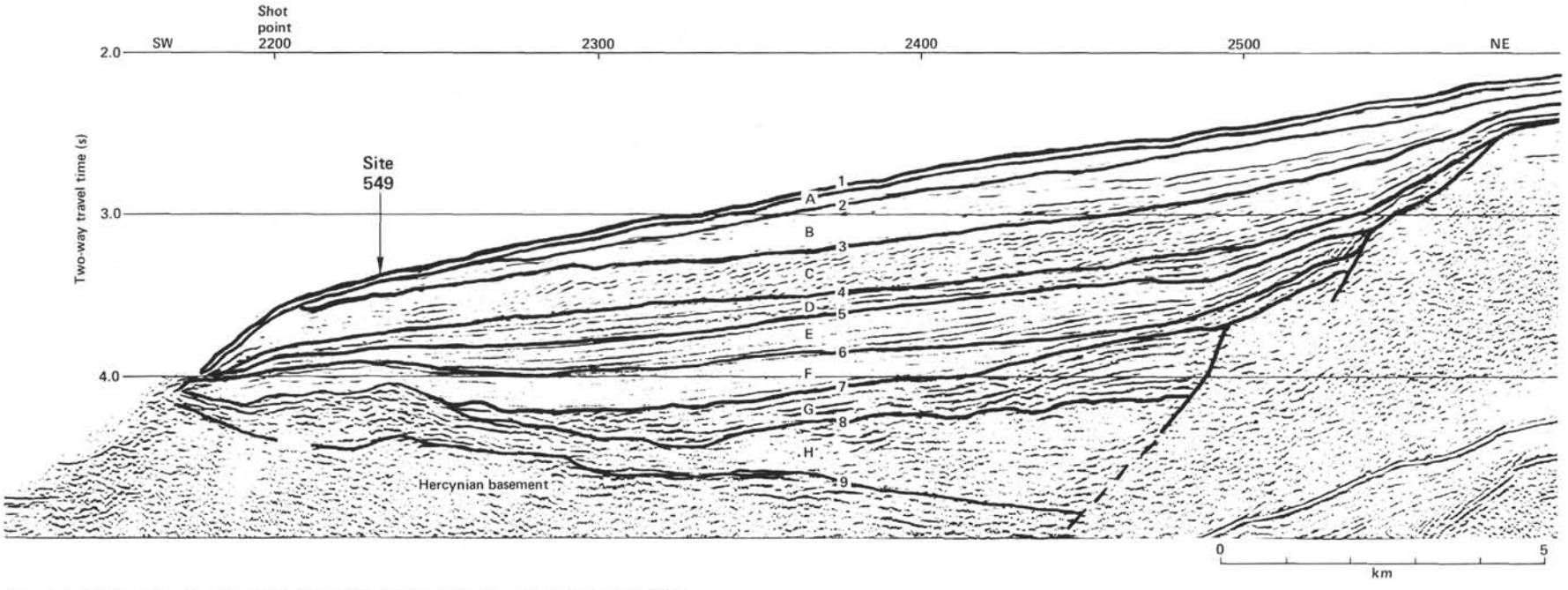

Figure 6. Major seismic sequences on profile CM 10 where it crosses near Site 549.

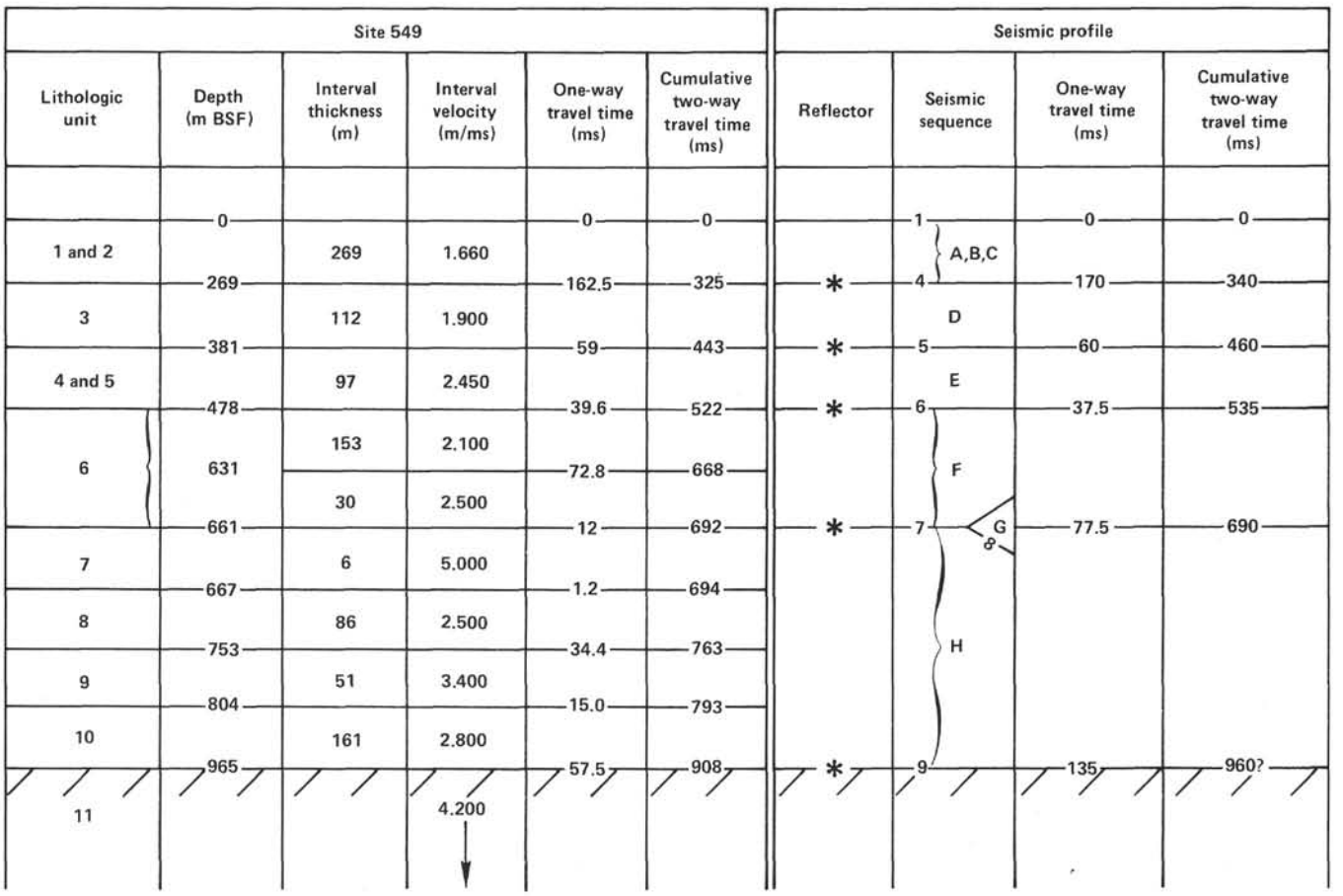

Figure 7. Relationship between physical properties of rock and sequences visible in seismic profile, Site 549.

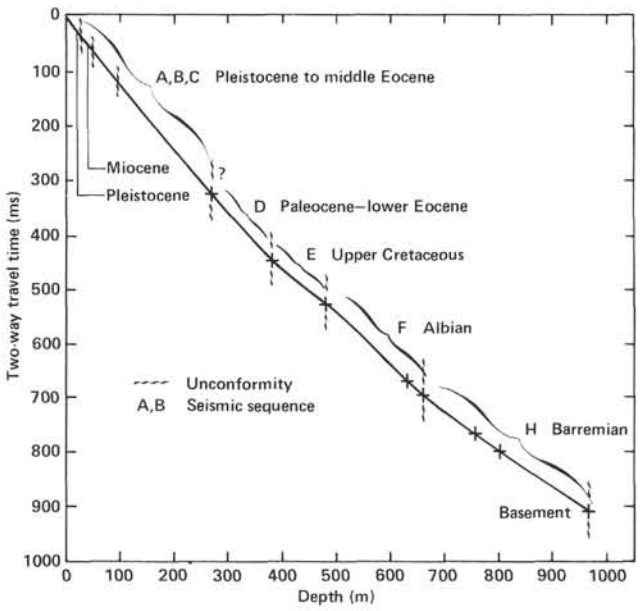

Figure 8. Two-way travel time versus depth, Site 549.

Seismic Sequences at Site 550

The three major sequences are easily recognized above the basement high at Site 550.

Sequence C is reduced to about 100 ms on the top of the basement high but thickens to 300 ms to the west and 400 ms to the east. Even though a strong reflector situated near the base of Sequence C to the west can be followed to the top of the high, it is probable that we missed a part of the oldest sedimentary section at Site 550. The contact with the oceanic crust is marked by a strong reflector. Another one is visible within the basement, dipping to the east. It could be either an interbedded sedimentary sequence or a pegleg resulting from a multiple reflection between the top and the bottom of the sequence. The top of Sequence C is also marked by a strong reflector, but only above the basement high. This indicates a higher impedance contrast between Sequences C and B on top of the high (where beds have been truncated) than on both flanks. The seismic line thus indicates that an important stratigraphic gap is present between Sequences C and B.

Sequence B is only slightly thinner on top of the structure than on the two flanks (about 250 ms versus 300 ms). Nevertheless there are some reflection truncations in the top part of Sequence B. There are several continuous strong reflectors in the middle of the sequence.

Sequence A displays only slight deformation above the basement high. One hundred ms above the base of the sequence there is a reflector that can be followed a long distance on profile IOS CM 11. Above this, a dis-

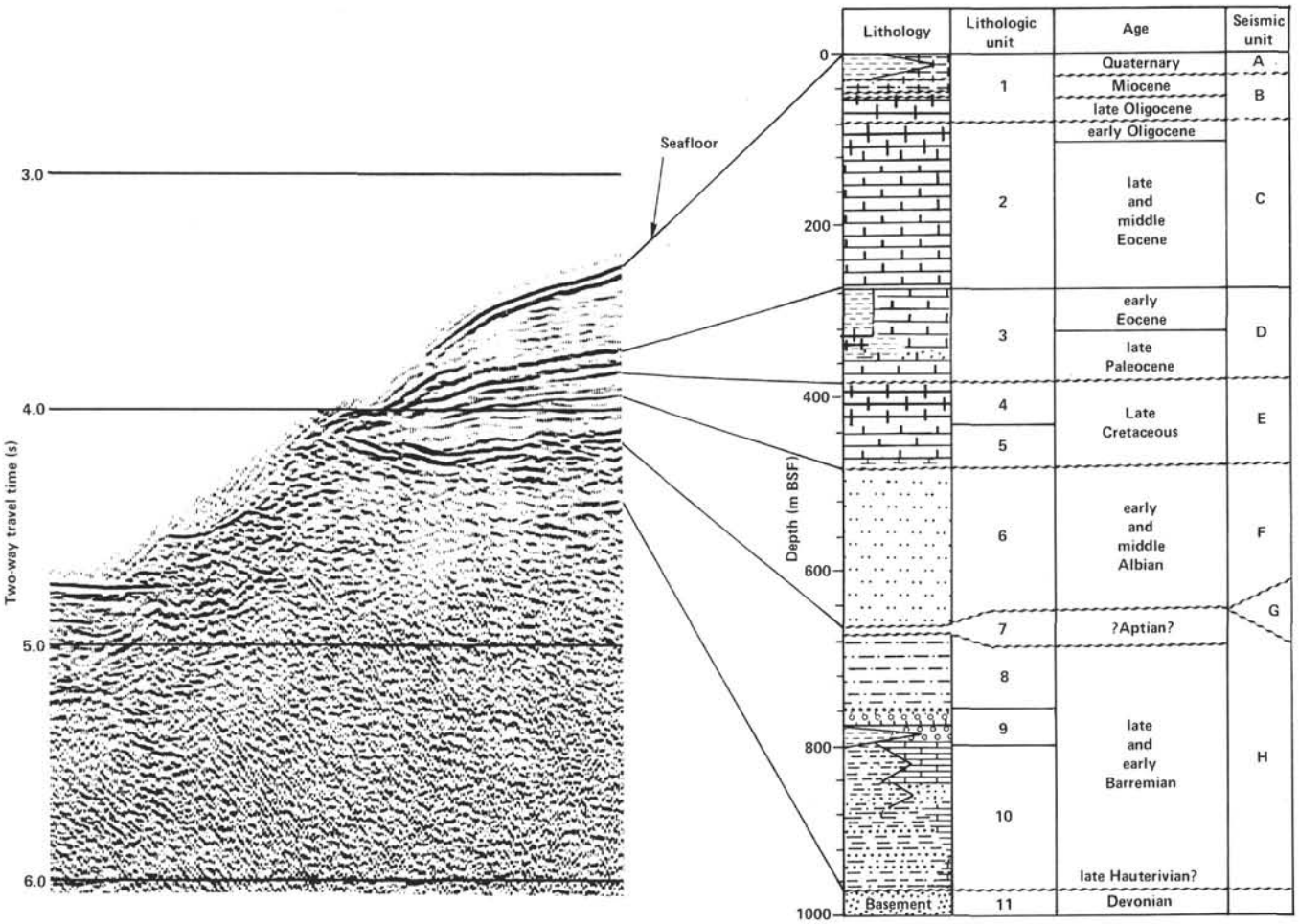

Figure 9. Correlation of core hole stratigraphy and seismic sequences at Site 549. Symbols used for lithology as defined in Explanatory Notes (this vol.). Small circles denote grainstones.

continuous reflector delimits the upper half of the sequence, where the seismic facies suggests a complex sedimentation pattern.

There are some uncertainties about the exact location of Site 550 on line CM 11 because the single-channel *Glomar Challenger* profile is hard to correlate with the migrated multichannel profile. Nevertheless, taking into account the water depth, we fixed the most likely location at shot point 1412 near a slight dip in the seafloor.

The two-way travel times from the seafloor to the sequence boundaries and main reflectors are as follows:

Sequence	Reflector	Two-way travel time (ms)	Reflector characteristics
	Seafloor	0	
A	A_1	140	Discontinuous
	A_2	260	Continuous
	Boundary	330	Continuous with truncation
B	B_1	430	Close together
	B_2	460	
	B_3	500	
	Boundary	580	Continuous with truncation
C			
	Basement	690	Continuous

Depth–Travel Time Relationship at Site 550

A good sonic velocity log recorded in Hole 550B facilitates the establishment of the depth–travel time relationship at this site. Integrated travel time for each distinctive interval except the top 93 m was read directly from the sonic log. For the top section (0–93 m BSF), a mean velocity of 1.6 km/s was used. Two-way travel times from the seafloor were then calculated and compared with the two-way travel time to sequence boundaries and main reflectors, with the results shown in Figure 13. Depth–travel time relationships are shown on Figure 14. There is a good correspondence between boundaries of seismic sequences and important unconformities documented at the site. A systematic small difference of about 10 to 15 ms is apparent between travel times in the hole and in the seismic profile. This may be due to either a difference between the supposed and the exact location of the hole or slightly higher interval velocities obtained from seismic reflection than from the sonic log.

Results

Correlation between the seismic reflection profile and the stratigraphy of the hole yields the following integrated stratigraphic synthesis (Fig. 15).

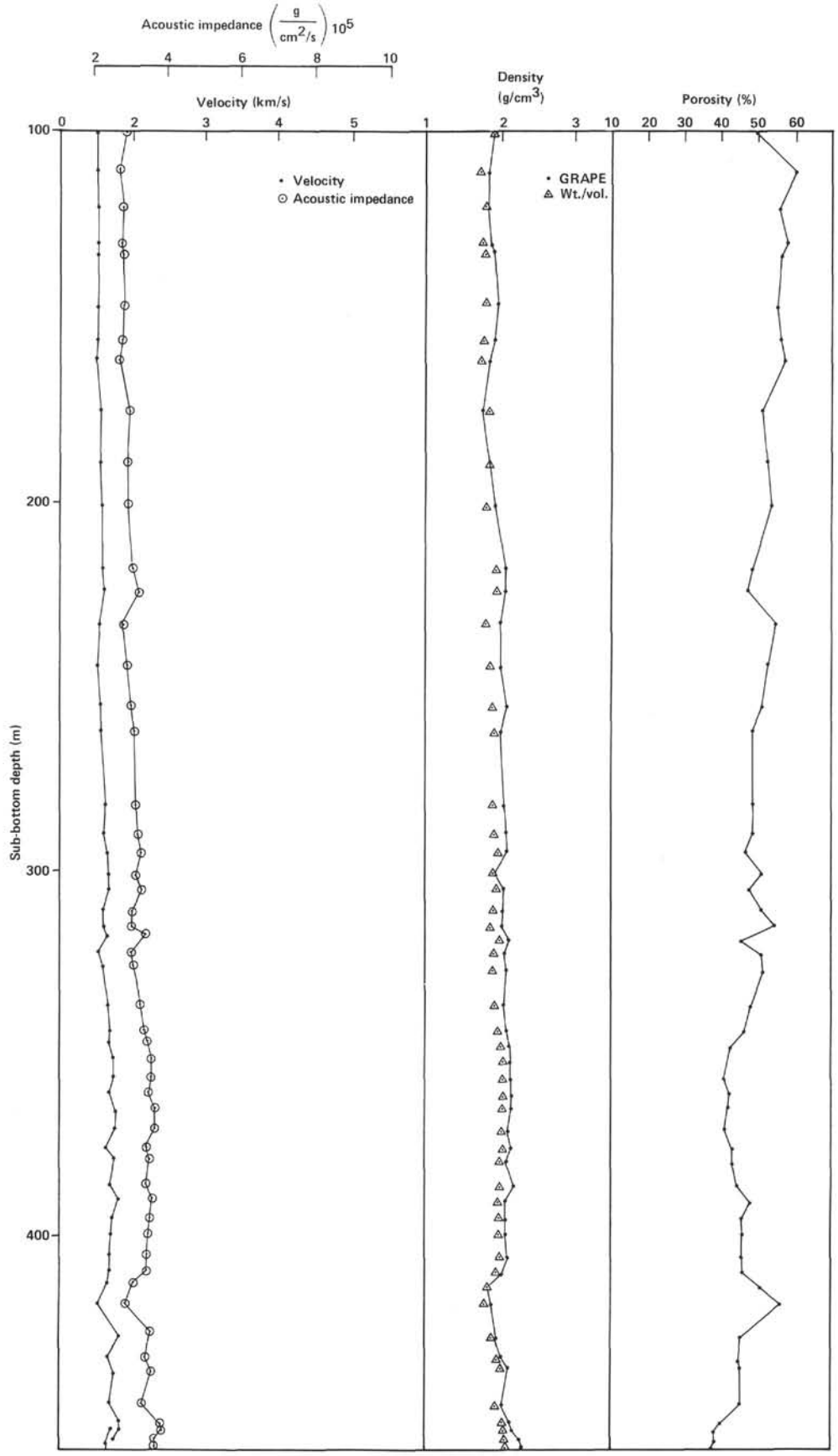

Figure 10. Physical properties, Site 550.

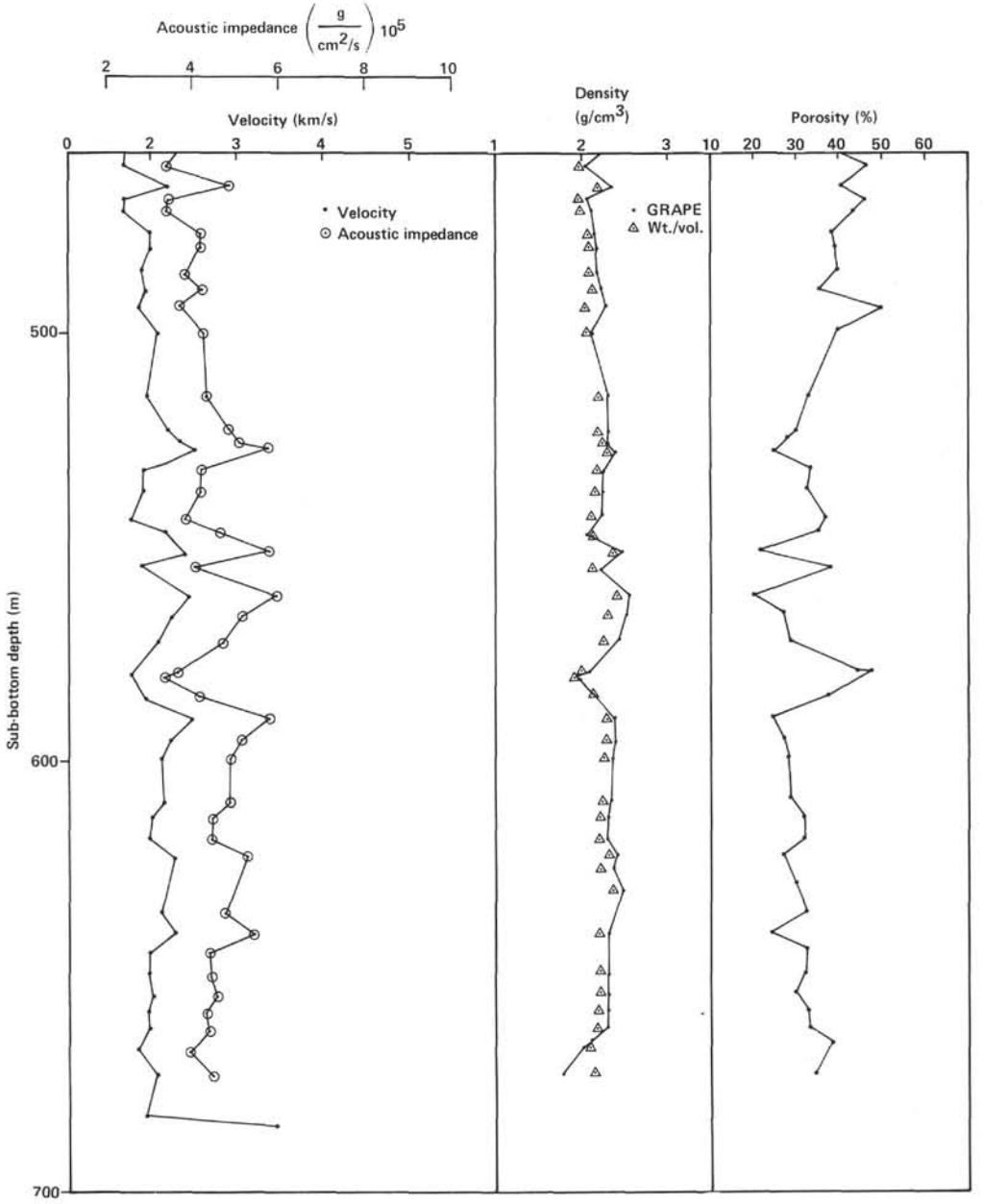

Figure 10. (Continued).

Seismic Sequence A corresponds to the interval from the seafloor to an important unconformity and/or a condensed section that resulted from intense dissolution between (?)upper/lower Oligocene and lower Eocene strata (i.e., Sequence A-lithologic Unit 1). Reflector A_1 may correspond to the base of the Miocene slumps within the lower Pliocene. Reflector A_2, which is continuous, very probably marks the unconformity observed in the middle Miocene section.

Seismic Sequence B corresponds to the interval from the lower-middle Eocene to the Maestrichtian–upper Campanian (lithologic Units 2 and 3). Its base is an unconformity and/or condensed section encompassing the lower Campanian to upper Cenomanian. The close reflectors B_1, B_2, B_3 correspond to a succession of lithologic changes. B_1 indicates a change from calcareous mudstones to siliceous mudstones in the upper Paleocene. B_2 signifies a change within the upper Paleocene from siliceous mudstones to chalks and may be associated with an unconformity. B_3 reflects a change from calcareous mudstones in the Danian to nannofossil chalk of the Maestrichtian.

Seismic Sequence C corresponds to the interval containing the lower Campanian to upper Cenomanian section and the middle Cenomanian to late Albian chalks that rest on the oceanic basement (lithologic Units 4 and 5). The seismic reflection profile shows that on both flanks of the basement high, Sequence C thickens con-

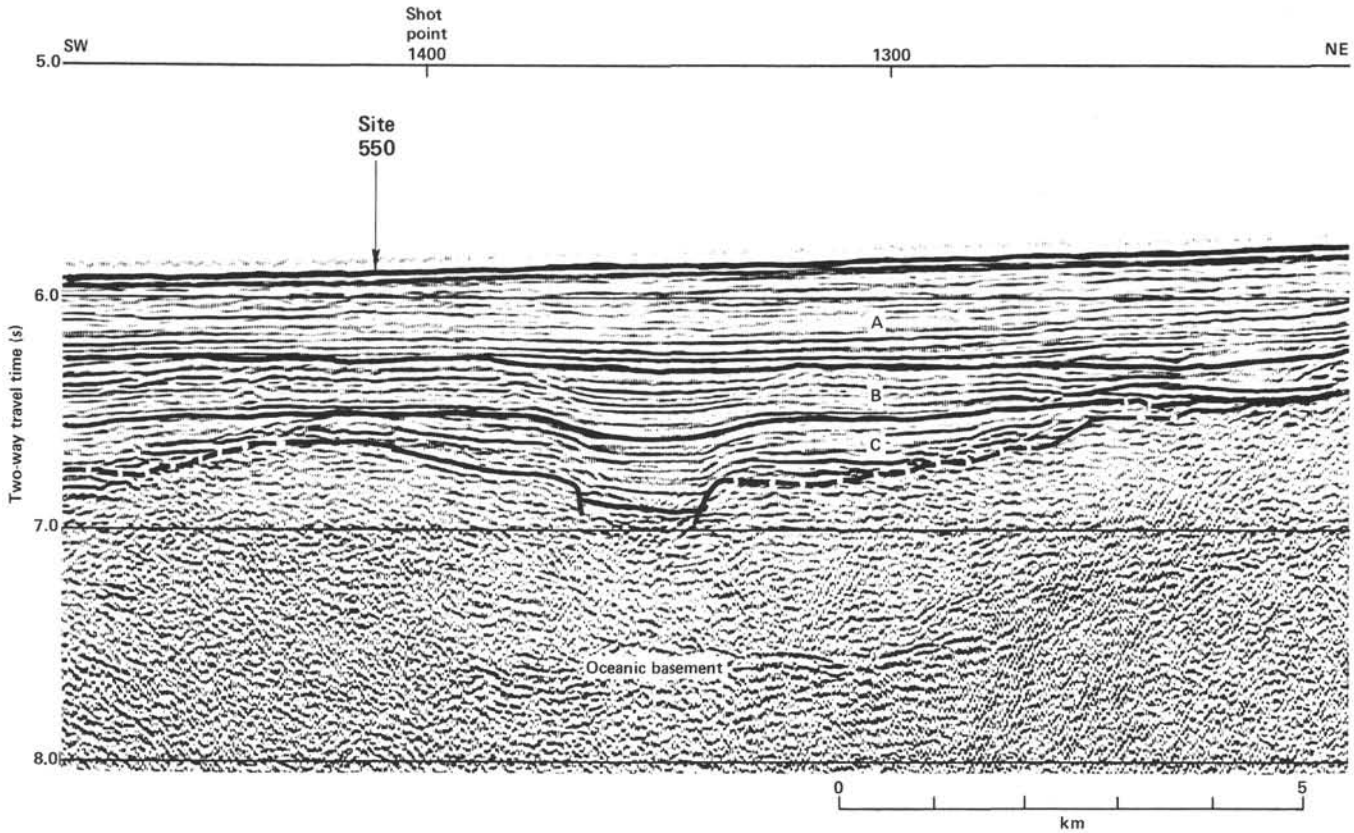

Figure 11. Distribution of seismic sequences along seismic line CM 11 as it crosses near Site 550. Note that sediments in the fault block 3 km northeast of Site 550 appear to be older than the oldest sedimentary strata at the bottom of Hole 550.

siderably in the Campanian and middle Cenomanian interval. A part of the oldest sediments that exists in the graben east of Site 550 may also have been missed.

SITE 551

Physical Properties

Measurements of sonic velocity, bulk density from GRAPE special 2-minute count, wet-bulk density, and porosity–water content were made on 10 sediment samples from Site 551. Velocities vary from 1.56 to 1.975 km/s. This is in accordance with the mean velocity of 1.77 km/s (seismic reflection travel time) for the 142 m of sediments penetrated.

On basalts, 20 velocity measurements were made on half-cores and plugs. For these plugs a "corrected" wet-bulk density was determined by GRAPE special 2-minute count. Samples were kept saturated for further onshore studies.

All measurements are listed on Table 1. Velocities of basalts are plotted in Figure 16. They range from 3.9 to 55 km/s, but most values cluster between 4.5 and 4.9 km/s.

Correlation of Seismic Profiles with Drilling Results

General Setting

At Site 551, we intended to document the sedimentary cover and the basement on the most seaward edge of the Goban Spur near its contact with well-defined oceanic crust. Prior to drilling, this location was thought to occupy the deepest tilted block of the continental crust that is truncated by an erosional surface. Oceanward, the block is bounded by a steep scarp 400 m high (Fig. 17). The top of the block (beneath Site 551) is 1500 m higher than the adjacent oceanic crust (5600 m depth) and about 1000 m lower than the block beneath the Pendragon Escarpment (3100 m depth).

On seismic profile CM 10, sediments are about 1100 m thick at the foot of the scarp; this is a thicker section than on line CM 11, where Site 550 was located. Generally, profile CM 10 displays the same major seismic Sequences A, B, and C as are present on CM 11. The nearly transparent Sequence C, of mainly Late Cretaceous age, is clearly displayed, having a strong reflector at the base corresponding probably to the top of upper Albian to middle Cenomanian strata.

Sequence B, of Maestrichtian to early Eocene age, contains continuous strong reflectors, but it seems to be thinner than Sequence C. Sequence A is better developed, having in its lower half the characteristic seismic facies previously noted on Goban Spur and corresponding probably to the middle–upper Eocene and perhaps part of the Oligocene section. Several reflectors onlap the seaward-facing escarpment adjacent to Site 551.

Landward between Site 551 and the Pendragon Escarpment (shot points 1540 to 1950), a large depression is filled by horizontally bedded sediments with a maxi-

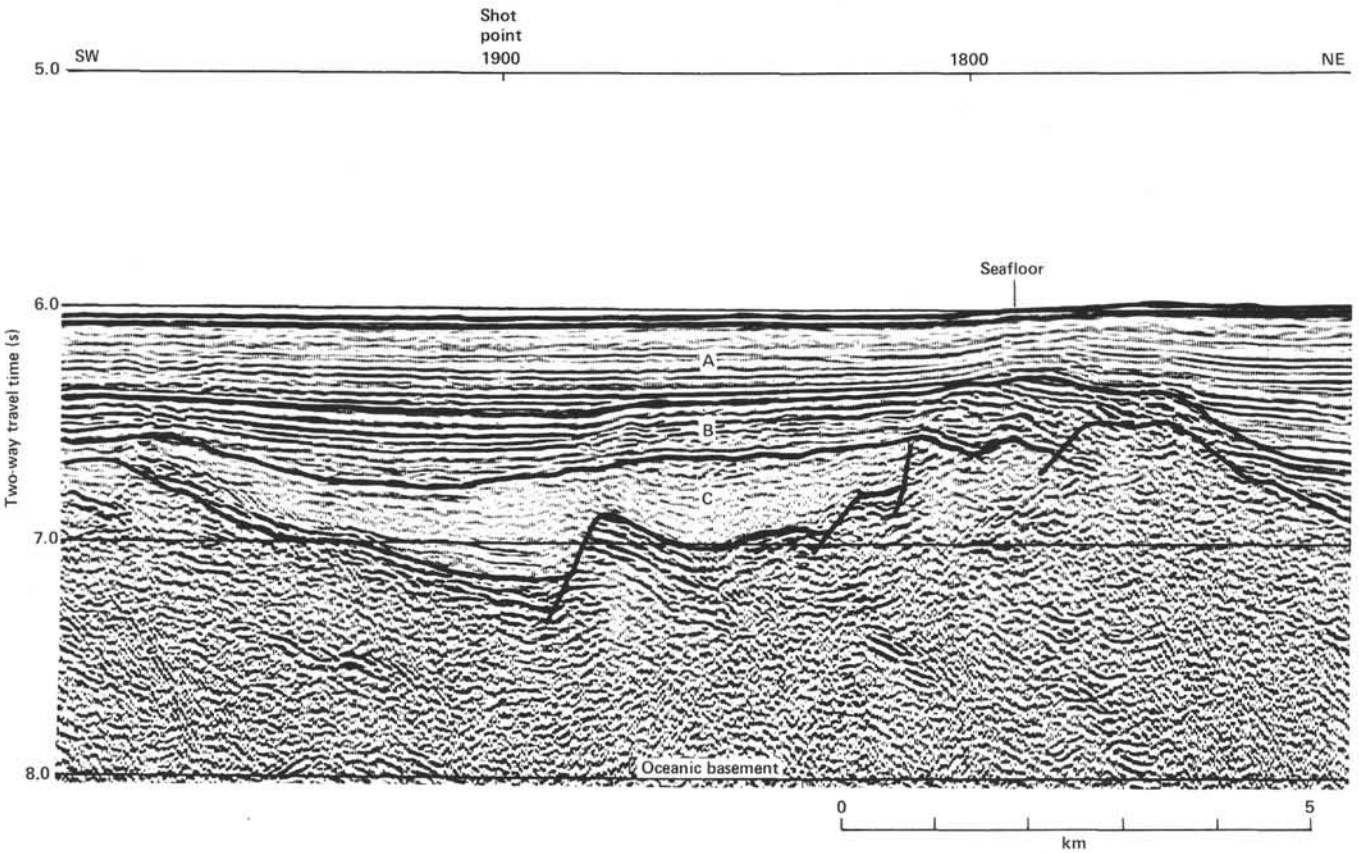

Figure 12. Distribution of seismic sequences along seismic line CM 11, approximately 25 km southwest of Site 550. Note complex faulting within upper part of oceanic basement.

mum thickness of 1400 m (near shot point 1820). As a whole the seismic facies of this fill is somewhat intermediate between the area of Site 549 and the abyssal plain. Most of the sequences (A–D) are horizontal and onlap both margins of the depression and thus clearly postdate the rifting phase of the margin. However the oldest sequence (E) fills a small graben, and it thickens to the northeast, suggesting that it may be a synrift deposit (Aptian?). Correlation with the area of Site 549 would suggest the existence of about 150 m of Albian (D) above this, covered by about 400 m of chiefly Upper Cretaceous strata (C). The upper layers of Eocene (B) and Oligocene to Quaternary age (A) are up to 700 m thick. Here again, the characteristic facies of the Eocene is present. These sequences thin on the basement high (shot point 1500) from about 400 m at its landward edge to zero at its oceanward edge. On the landward edge of the high, the seismic profile shows a feature somewhat similar to a buried carbonate buildup.

Below the horizontal sedimentary infill there is no evidence that the characteristic synrift deposits dip landward. No coherent reflection appears below the high itself.

Comparison with the Drilling Results

Only 142 m (instead of the 200 m expected) of an incomplete sedimentary section (Pleistocene to upper Cenomanian) was encountered at Site 551; the rest of the drilled section consists of basaltic pillow lavas and flows. The top of the basalt appears to be marked by a strong reflector at 160 ms. This would give a more reasonable velocity (1.775 km/s) for the overlying sedimentary section.

Within the basement high, coherent reflectors are visible, but they cannot be directly correlated landward with the thick basin fill. The upper Cenomanian chalks found at Site 551 must be correlative with beds deep in the adjacent depression.

The finding of relatively deep-water sediments on top of the basalts (lower bathyal?–upper Cenomanian) appears to exclude the existence of a carbonate buildup on the basement block. We suggest that this mound-like feature is part of a previous oceanward slope (chiefly of Eocene age) that was subsequently buried by Neogene and Quaternary strata. The mound is mainly defined oceanward by a strong dipping reflector and landward is marked only by diffractions and a change in character from well organized to chaotic reflectors.

Site 551 has brought new insight to the interpretation of the seismic reflection profiles in the area intermediate between the well-defined rifted margin and ocean crust. Re-examination of magnetic and gravity data combined with the drilling results leads to the conclusion that the basement high beneath Site 551 is transitional between

Site 550						Seismic profile			
Lithologic units	Depth (m BSF)	Interval thickness (m)	Interval velocity (m/ms)	One-way travel time (ms)	Cumulative two-way travel time (ms)	Reflector	Seismic sequence	One-way travel time (ms)	Cumulative two-way travel time (ms)
	0				0			0	
1a		93	1.610	57.7				70	
	93				115				
		36.5	1.780	20.5					
	129.5				156	* A_1			140
		38.5	1.830	21.0					
	168.0				198		A		
1b		28.0	1.860	15.0				60	
	196.0				227				
		68.7	1.950	35.5					
	264.7				298	* A_2			260
		44.8	2.000	23.0				35	
	309.5				344	**			330
		26.5	1.800	14.5					
	336.0				373				
		26.5	2.000	13.5				50	
2	362.5				400				
		44	1.910	23.0					
	406.5				446	* B_1			430
		26.5	1.800	15.0			B	15	
	433.0				476	* B_2			460
		31.7	2.050	15.5				20	
	464.7				507	* B_3			500
3		41.3	2.580	16.0					
	506.0				539			40	
		65.8	2.250 to 3.000	26					
	571.8				591	**			580
4		23.2	2.000	11.5					
	595.0				614				
		33.7	2.475	13.6			C	55	
5	628.7				641				
		55.3	2.300	24.0					
	684.0				689	**			690
6									

Figure 13. Relationship between physical properties of rock and sequences visible in seismic profile, Site 550. Particularly strong reflectors are marked by double asterisks.

true continental crust and true oceanic crust (see Scrutton, this vol. and Masson et al., this vol.). This feature has many similarities with marginal highs often described at ocean/continent boundaries, which are emplaced in the axes of the rift systems just before the separation of continents.

REFERENCE

Vail, P. R., Mitchum, R. M., Todd, R. G., et al., 1977. Seismic stratigraphy and global changes of sea level. *In* Payton, C. E. (Ed.), *Seismic Stratigraphy Application to Hydrocarbon Exploration.* Mem. Am. Assoc. Pet. Geol., 26:49–205.

Date of Initial Receipt: May 29, 1984
Date of Acceptance: June 8, 1984

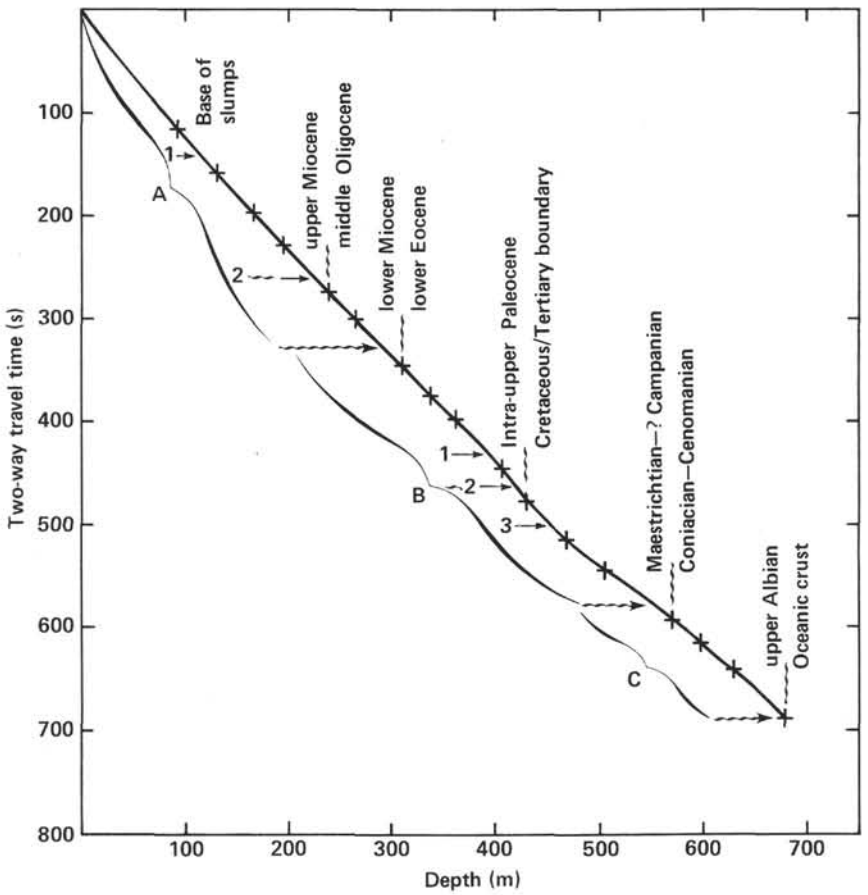

Figure 14. Two-way travel time versus depth, Site 550.

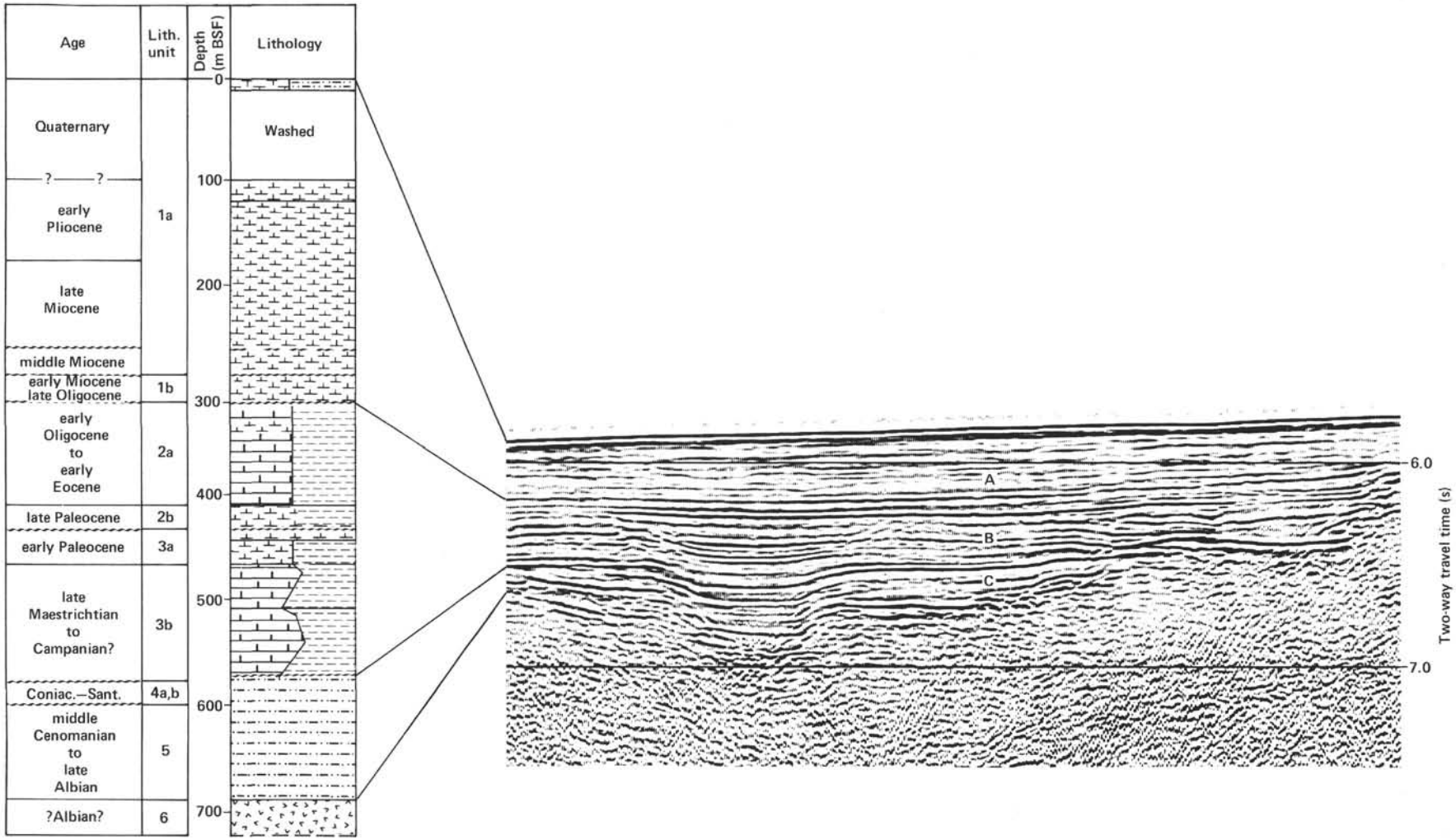

Figure 15. Correlation of seismic sequences with drilled stratigraphy at Site 550. Symbols used for lithology as defined in Explanatory Notes (this vol.).

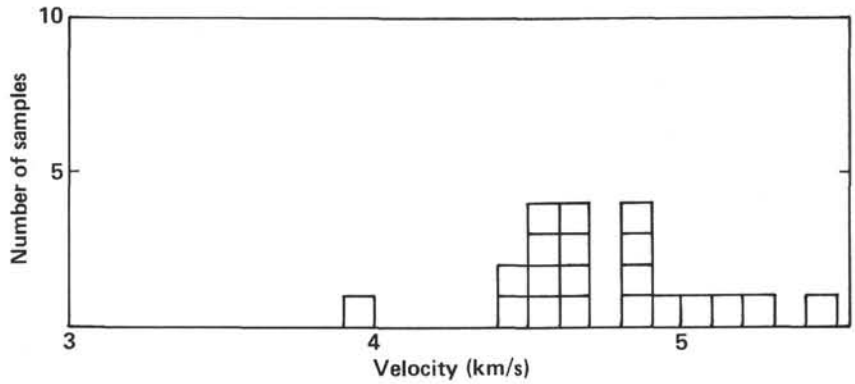

Figure 16. Basalt velocities, Site 551.

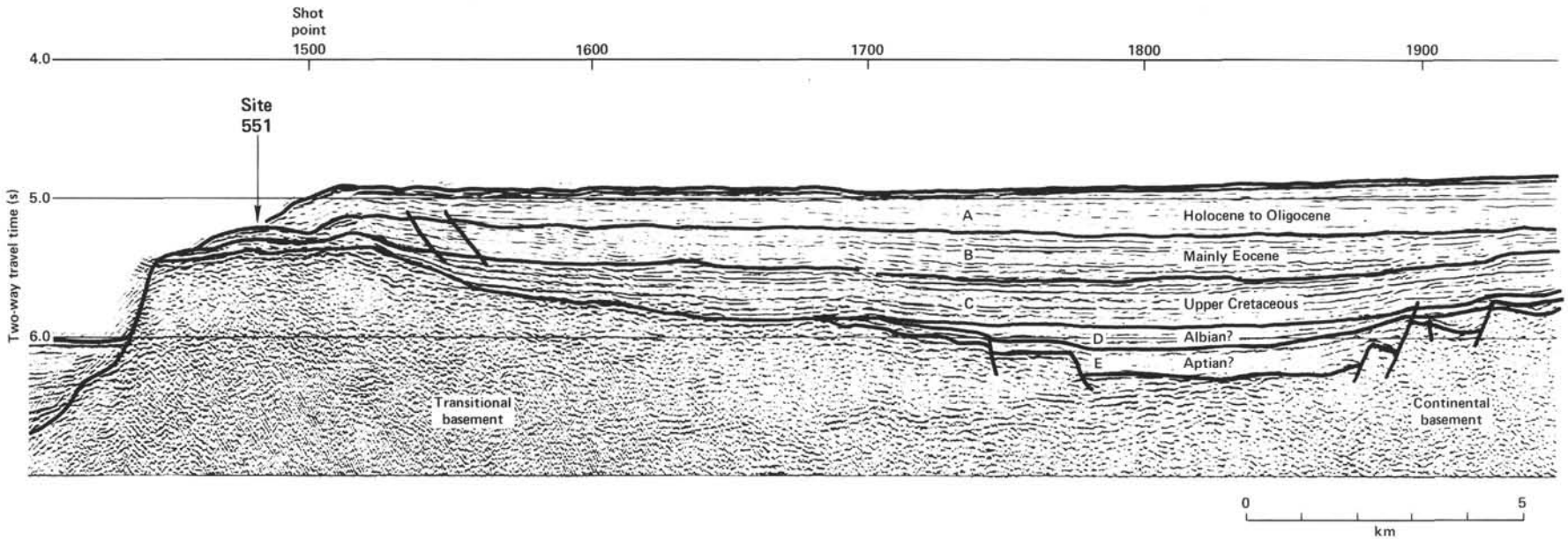

Figure 17. Segment of seismic profile CM 10 that crosses Goban Spur near Site 551. Correlation of seismic sequences with the drilled section is shown at the site and in the basin landward of Site 551.